#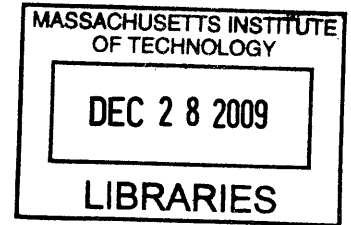 Design and Development of High Precision Five-Axis Positioning System for Roll-to-Roll Multi-Layer Microcontact Printing

by

Paolo Baldesi

Laurea in Ingegneria Meccanica
Sapienza University of Rome, 2007

Submitted to the Department of Mechanical Engineering in partial
fulfillment of the requirements for the Degree of

Master of Engineering in Manufacturing   **ARCHIVES**

at the

MASSACHUSETTS INSTITUTE OF TECHNOLOGY

September 2009

Signature of Author ....
Department of Mechanical Engineering
18 August 2009

Certified by ....
David E. Hardt
Professor of Mechanical Engineering
Thesis Supervisor

Accepted by ....
David E. Hardt
Chairman, Departmental Committee on Graduate Studies
Department of Mechanical Engineering

Design and Development of High Precision Five-Axis Positioning System for Roll-to-Roll Multi-Layer Microcontact Printing

by

Paolo Baldesi

Submitted to the Department of Mechanical Engineering on 18 August, 2009,
in partial fulfillment of the requirements for the
Degree of Masters of Engineering in Manufacturing

Abstract

Microcontact printing is based on the use of elastomeric stamps to transfer ink onto a substrate taking advantage of the self-assembly process. Features as small as 300nm can be easily printed over an extended area. The accuracy and the speed of the process make it suitable for many industrial applications in areas such as the manufacture of flexible displays and electronics.

In 2008, a group of MIT mechanical engineering students built a prototype machine that demonstrated the advantages of the roll-to-roll paradigm in terms of high throughput, convenient material handling and conformal contact propagation. The prototype machine, although characterized by defects such as air trapping at very high speed, was able to print at speeds as high as 400 fpm with contact times of 7 ms, over an 8"x 8" substrate area. This year, an improved quality printing output and multilayer printing process were set as goals. To achieve the objectives, a device that could cast a flat stamp with little variance was designed and machined. A high precision wrapping system was designed and fabricated. Finally, a high-precision positioning system was introduced to compensate for misalignment in the multi-layer printing process.

This thesis describes the design of a five-axis high-precision positioning system to control the print roller along five degrees of freedom. Using flexures and micrometer heads as principal position control devices, the print roller can be positioned and oriented with high repeatability, 2.5μm accuracy, 2.5μm resolution, and the calibration showed that, in the worst case, the coupling among axes is limited to the 8%. Moreover, experimental results demonstrate that the new stamp casting method can accomplish $\pm$16μm flatness with thickness of 1194μm and that the innovative wrapping process ensures alignment of the backing plate with respect to the print roller with less than $\pm$75μm absolute misalignment. Consequently, using the upgraded roll-to-roll machine and the newly developed wrapping and stamp fabrication processes, deformation of the printed output is limited to an average of 3.8%. Finally, the multi-layer printing process was tested and a $\pm$75μm misalignment was achieved between two layers.

Thesis Supervisor: Dr. David E. Hardt
Title: Professor of Mechanical Engineering

Acknowledgements

First, thanks to my wonderful teammates: Charudatta Datar, Yang Wenzhuo, and Yufei Zhu. Their hard work and bright ideas helped carry this project. Each of us brought something unique and interesting to the table, and our minds and ideas melded and mixed into a fantastic team.

Many thanks also to my advisor Dr. David Hardt for his guidance, insight, and open door.

Thank you to everyone at Nano Terra for being friendly, professional, and ever so helpful to four manufacturing engineers thrown into a chemistry laboratory.

A million thanks to Shih-Chi. He and Nano Terra put an incredible amount of trust in us, and that is truly what made this a worthwhile experience, both for us and, hopefully, for Nano Terra.

Last, and definitely not least, thanks to my family for their patience and continuing support of everything and anything I pursue.

Table of Contents

List of Figures

9

List of Tables

CHAPTER 1 – Introduction

1.1 Motivation

Currently, nanostructures are commonly fabricated using techniques such as photolithography, electron-beam writing and X-ray lithography. Although these methods are proven technologies that provide high-quality outputs, there are inherent problems. These techniques are generally expensive, slow, and the production of large patterns is difficult. Micro-contact printing (μCP) is a promising technology in which a patterned elastomeric stamp is used to transfer patterns of self-assembled monolayer (SAMs) onto a substrate by conformal contact printing. In 2008, a group of MIT students developed a high throughput, low cost roll-to-roll (R2R) printing technique into micro-contact printing, achieving good results. They also built a prototype machine to realize the whole process in the speed of 400 feet per minute while maintaining good quality outputs.

However, the last year's machine is only limited to printing octadecanethiols, an organic ink, on gold substrates where the self-assembly characteristics (see section 2.1) of these media could tolerate big range of pressure variance applied on the substrate. Therefore, if the micro-contact printing is applied into some other media where self-assembly characteristics do not exist, a highly uniform pressure along the substrate will be critical to the quality of outputs. The pressure of previous prototype machine is provided by the contact of the print roller and the impression roller. The uniform roundness and straightness of the rollers is the key to the uniform pressure along the contact area. Meanwhile the parallel contact between the impression roller and the printer roller is also very important. Therefore, if we can fabricate the print roller with the variance less than a few microns and the contact between the impression roller and the printer roller has good parallelism with high repeatability, then the roll-to-roll micro-contact printing technology could be easily applied to various printing media.

The printer roller consists of central shaft, sleeve, the backing plate and the stamp (see section 2.2). The uniform thickness of the stamp is the most critical component of the uniform roundness of the print roller. Currently, there is no standard process to fabricate the stamp with the thickness variance of a few microns, therefore, the repeatable, reliable and manufacturable stamp fabrication process is also highly desired.

Another limitation of last year's project is that the registration of multiple layers on a flying substrate was not considered; only monolayer could be printed using the prototype machine. However, in the industry, multi-layer printing is required, which means to print another layer on the substrate with patterns. At present, the commercial printing industry, where multi-layer printing is very common and popular, can only achieve a resolution of 40 microns. Thus, such technology can hardly be applied to multi-layer printing where the pixel size is less than 40 microns. If multi-layer printing with the resolution of 1 micron could be demonstrated by upgrading the previous prototype machine, there will be a significant impact in the printing industry.

Research was funded by and in cooperation with Nano Terra Inc, a Cambridge, Massachusetts company that specializes in Soft Lithography.

1.2 Problem Statement

The primary objective of this project is to address the limitations of the previous prototype machine in related to the potential manufacturing of printed electronics using micro-contact printing technique within the soft lithography (SL) field.

At first glance, the main goals of this project can be split in two major areas:

1. Improve the printing quality, upgrading the R2R system built by the MIT students in 2008; in particular this goal will be achieved by designing and fabricating an interchangeable stamp on the roller that allows a quick replacement of the stamp once it is used up, without losing of alignment. This goal is achieved by performing three key steps:

   o Design of an interchangeable stamp.
   o Fabrication and demonstration of interchangeable stamp.
   o Test results providing data on distortion, and alignment.
   o Budget estimate for manufacturing applications.

2. The second main goal of the project is to improve the overall R2R system. This task is achieved by executing the following steps:

   o Redesigning and implementing the impression roller system.
   o Designing process for multi-layer printing
   o Designing a high precision positioning system.
   o Test results providing data on distortion and alignment.
   o Budget estimate for manufacturing applications.

1.3 Primary Analysis

We considered the two major goals of the project, namely, fabricating a very flat stamp and then wrapping it around the print roller, and proving that micro-contact printing can be used for printing multiple layers with alignment.
In order to fulfill these goals, our approach consisted of accomplishing the followings:

1. Flat stamp fabrication. To achieve this, a new method was developed to fabricate the stamp using a molding process, to ensure a flat and defect-free stamp.

2. Wrapping the stamp with backing plate onto the roller with alignment and repeatability. The goals of this process were to wrap the stamp while maintaining alignment, and developing a repeatable process; and to maintain uniform roundness of the stamp after wrapping. To achieve this, after looking at a lot of options, we decided to use a magnetic cylinder, and a pin-slot system to grab the edge of the backing plate. We also considered a fixture system to wrap the stamp with backing plate on the cylinder.

3. Ensuring the roundness of assembled print roller within 4 microns tolerance. With proper wrapping method, minimal and uniform printing pressure could be achieved and hence realized good printing quality.

4. Redesigning the impression roller system to improve its repeatability of parallelism. In this process, we built up error budget model, found out the constraint to the repeatability of the impression roller system and then updated the system.

5. Designing a high precision position system to control the print roller position and orientation. This step was fundamental to improve the quality of single layer printing as well as the multiple layers printing.

6. Printing using the updated machine and comparing results that achieved by last year's group. After we qualified the wrapped stamp and impression roller system, we mounted the new roller onto the current machine, to get a direct comparison of print quality.

7. Printing multiple layers as a proof of concept. This was an independent step, to prove that micro-contact printing can print multiple layers on a single substrate with minimum misalignment.

13

1.4 Scope

Our project only dealt with micro-contact printing with PDMS as the stamp and 300mm wafer as the master. We focused on printing thiol onto gold-coated substrates. This scope allowed us to decide the dimensions of our design based on available materials. The mature printing mechanism also allowed us to verify our designs without disturbance of different printing conditions.

For multi-layer printing, the initial purpose was to use rigid and transparent material (glass) as the substrate to print two layers using the same stamp to print twice. Later on, the scope switched to using updated R2R machine to print two layers with the same stamp in order to demonstrate what is the best alignment that can be achieved using current Roll-to-Roll technology. In order to achieve this target, precise control of the printer roller on its alignment is required and we assumed the motion of the flexible substrate is self-aligned across the printing direction.

1.5 Task Division

This thesis is based on a team project executed as part of the Mechanical Engineering Master of Engineering in Manufacturing Degree Program. The team members were:

Wenzhuo Yang has researched and determined the measurement methods for cylinder roundness, tolerance of stamp fabrication parts as well as the print quality of output features. He designed the measurement structure and analyzed the data obtain from both measurements. In addition, he worked with Yufei Zhu on the upgrade of impression roller system and multi-layer printing process design.

Paolo Baldesi has designed the high precision positioning system to control the position of the print roller. He calibrated the system and determined its performance. In addition, he worked with Charudatta Datar in developing an innovative wrapping process designing a new magnetic print roller. He also researched and designed the mechanism of growing UV-curable material onto cylinder directly.

Charudatta Datar has designed the magnetic roller, and developed the technique to attach and wrap the backing plate and PDMS stamp onto the print roller. He also worked with Paolo Baldesi in designing the high precision positioning system. In addition, he designed other components, compatible the high precision

positioning system, to mount the new print roller on the machine built by the MIT '08 team,.

Yufei Zhu designed and constructed the multi-layer printing machine. He also designed the stamp fabrication parts with Mr. Werner Menzi from Nano-terra Inc.

We collectively tested the machine and determined the quality of printing resulted from the machines. Since we were working on a common project, the first three Chapters of our individual theses are common. Moreover, Chapters 7, 8, and 9 are common for Paolo Baldesi and Charudatta Datar. Chapter 7 and 8 are brief introductions to Yufei Zhu, and Wenzhuo Yang's parts, while Chapter 9 discusses the conclusions of the project and possible future works.

CHAPTER 2 - Literature Review

This section summarizes the existing R2R machine developed in 2008 by Adam Stagnaro, Kanika Khanna, and Xiao Shen [4,20,21], introduced the technologies used in the machine, and described its structure, function, operation steps and the result achieved. Also some pioneering studies of the currently multi-layer printing technology were reviewed to enlighten our prototype design on current R2R machine. Finally, some popular and representative optical metrology systems are studied to search out proper methods for measuring the quality of the machine design and the print output.

2.1 Soft Lithography

Photolithography is a well-established micro-fabrication technology, being widely used to manufacture most integrated circuits. It is, however, limited to a feature size of about 100 nm owing to optical limitations. Technologies such as extreme UV lithography, soft X-ray lithography, electron-beam writing, focused ion beam writing, and proximal-probe lithography[1] are capable of manufacturing smaller features, however, they are limited by high cost and technology development.

Photolithography also has other limitations: it cannot be used on non-planar surfaces; it is incapable of producing three-dimensional structures, and it is not suitable for generating patterns on glass, plastics, ceramics, or carbon [1].

Thus, a family of techniques called as soft lithography, including, microcontact printing, replica molding (REM), microtransfer molding (mTM), micromolding in capillaries (MIMIC), and solvent-assisted micromolding (SAMIM) are emerging as prospective solutions to overcome some of the limitations of photolithography.

They offer a number of basic advantages, such as, little capital investment, and simplicity. Apart from these, soft lithography techniques can produce features smaller than 100 nm, with relatively simple technology, and they are not subject to optical limitations. They also offer flexibility in terms of surface material, and shape, overcoming some of photolithographic limitations.

These techniques are referred to as "soft lithography" because each technique makes use of flexible organic materials as opposed to rigid materials to achieve

pattern transfer to the substrate. Basically, these techniques involve the fabrication of an elastomeric stamp (typically made of Polydymethylsiloxane, PDMS), generating a replica of the pattern originally on a Silicon master, and using this stamp to print the pattern on a substrate using self-assembly.

Self-assembly refers to the spontaneous formation of molecules into organized structures by non-covalent forces. The resulting structure is highly uniform, defect-free owing to thermal equilibrium, and in the lowest energy form.
Self-assembled monolayer (SAM) is one such non-biological self-assembly system (see Figure 1 for its process). SAMs is used in soft lithography to transfer the pattern on the elastomeric stamp, onto the surface of the substrate using minimal contact pressure.
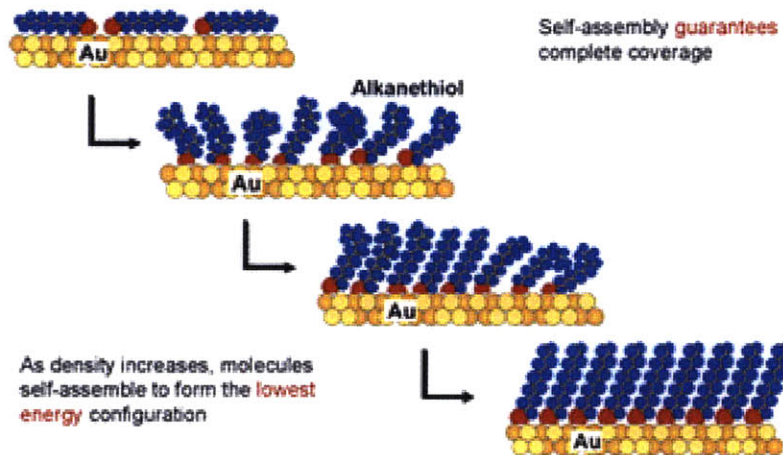
Figure 1: Illustration of The Self-Assembly Process[2].

We emphasize one of soft lithography techniques, microcontact printing, because we used this method throughout the project. This thesis does not describe the other methods.

2.2 Micro-Contact Printing

The micro-contact printing process involves transferring a pattern on an elastomeric stamp onto the surface of a substrate by the formation of a monolayer of ink, which can be used as resist in subsequent etching, or other steps. This process relies on SAM, in which it enables transfer of only a monolayer of ink to the substrate. This molecular level contact makes the process independent of excessive

17

ink being trapped between stamp and substrate, allowing significantly smaller sized (~ 50 nm) features to be printed onto the substrate.
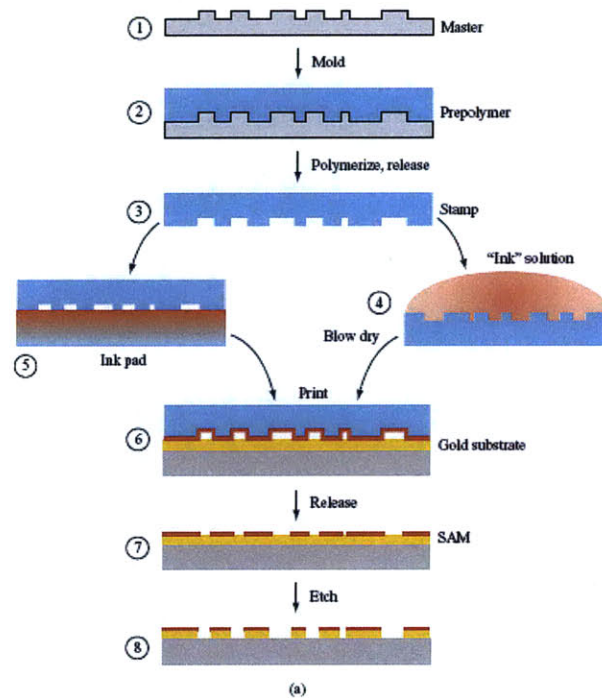
Figure 2: Steps Involved in Micro-Contact Printing [3].

The micro-contact printing process, as shown in Figure 2, involves, like all soft lithography techniques:

1. A master with the original pattern on it. This is typically a patterned Silicon wafer.
2. This pattern is then replicated on a PDMS stamp by casting or molding.
3. This PDMS stamp is then inked, by a couple of methods (using an ink pad, or pouring ink over the stamp).
4. Next, this inked stamp comes into contact with the substrate that is to be printed upon.
5. This contact enables the formation of a SAM of the ink on the surface of the substrate.
6. The stamp is released, and the SAM formed on the substrate is then used in subsequent etching steps to generate the required pattern on the substrate.

18

2.3 Existing Roll-to-Roll Equipment

The MIT'08 team's (Adam Stagnaro, Kanika Khanna, and Xiao Shen [4,20,21]) task was to take this demonstration to the next level, and prove that the paradigm would be competitive with commercial printing systems in at least one of the parameters - quality, rate, flexibility. The key goal of this MIT'08 project was to achieve Micro-contact printing at very high speeds (400 ft/min), on 8" wide coated substrate (web).
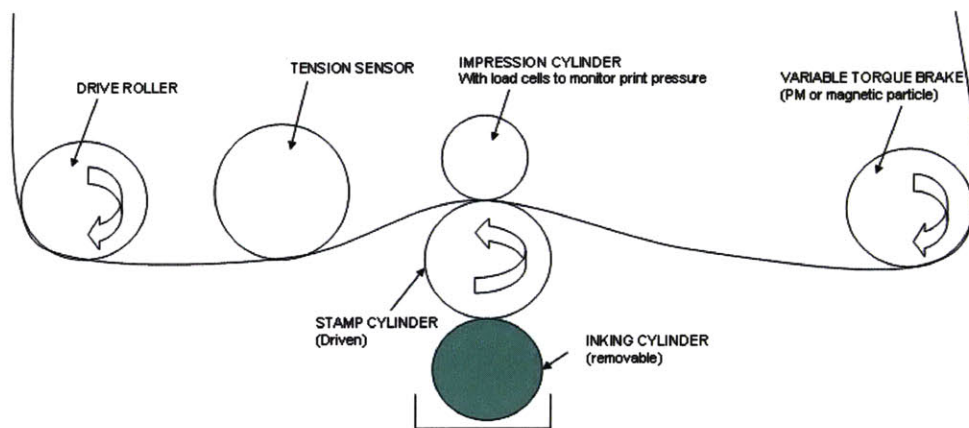
Figure 3: Concept of The Machine [4].

The concept of the machine is shown in Figure 3. The substrate was in the form of a web, driven through a set of rolls. A combination of open and closed loop using motors and clutches was used to achieve tension control.

The equipment can be divided into three modules:

1. Supply Module (to unwind substrate web).
2. Print Module (to ink, print, and apply pressure).
3. Collect Module (to rewind substrate web) [4].

The Figure 4 shows the layout of the machine, in terms of these three modules. The entire roller system is cantilevered about a common base plate. And Figure 5 shows the physical appearance of the R2R machine built by 08' group.
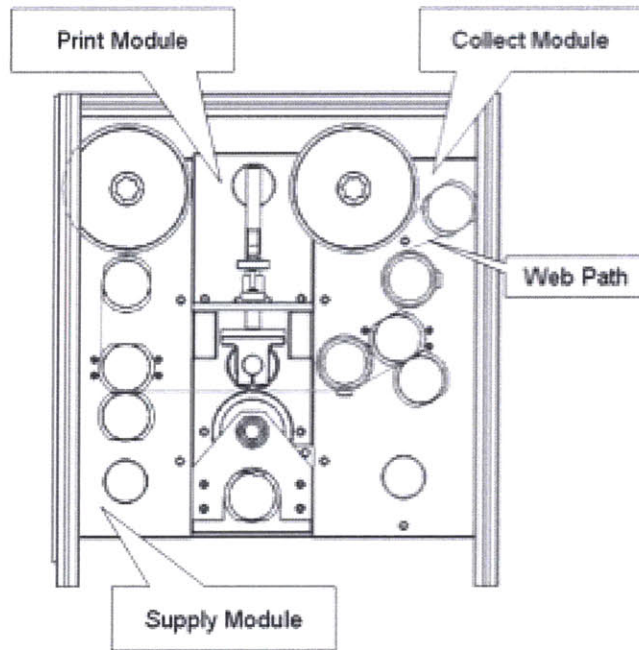
Figure 4: Layout of The Three Modules in The Equipment [4].

We shall not describe the operation of the machine in much detail, but will emphasize on the results of the print module only, as this was felt to have the most significant impact on the results, which also have been described in detail later in this document.
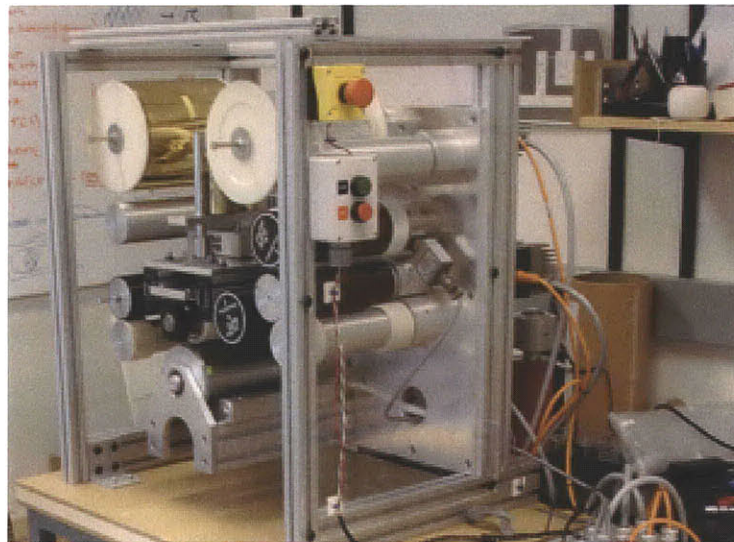
Figure 5: The R2R Machine Built in '08 [4].

A series of experiments were designed and conducted to test the printing quality. Below is a summary of relevant results [4]:

1. Neither printing pressure nor speed was found to have a significant effect on spatial distortions and pattern dimensions in the range of settings we used.
2. It is possible to print a robust etch-resisting SAM at very high speeds (400 ft/min, unit area contact time ~ 5ms).
3. At very high speeds (400ft/min), some systematic air trapping was observed
4. The alignment of the stamp on the backing may have a significant effect on distortion patterns.

These results have formed the basis for our project. Improvements in the following were seen as critical to improving the printing quality:

o Alignment of the stamp on the backing, and therefore on the print roller.
o Fabrication of a flat stamp.
o Precision in the web handling system of the equipment.

2.4 Stamp Casting Machine

Stamp fabrication is essential to improve the quality of printing. Micro-contact printing requires precise transfer of patterns with minimum distortion and maximum yield. In addition, the stamp needs to maintain an exactly complementary pattern to the master, and it should avoid distortion during printing.

PDMS as the material for stamp has a low Young's modulus; therefore, under tension or external force, the PDMS will distort and result in a distorted pattern. In previous projects, PDMS has been cast onto a rigid backing plate. The backing plate is treated with a plasma and surface treat chemicals to increase its adhesion to PDMS, and the force between this backing plate and PDMS is firm enough that little relative motion between the stamp and backing plate will happen. Thus, the backing plate with PDMS minimizes distortion when wrapping the stamp onto the print roller.

With the consideration of cost and efficiency, large stamps are desired for production. In common practice, round wafers (150mm, 200mm and 300mm size) are used as the master and etched out negative pattern on the SU-8 layer on the master. This photo-resist will directly contact PDMS during the practice, thus

21

caution should be made in order not to destroy the pattern on the master. The size of the stamp is limited by the size of wafer. In this project we targeted 300mm wafer as our master and explored the problems including distortion, uniformity, peeling force from master and repeatability with the capability of scaling in manufacturing.

In previous research at Nano-Terra LLC, the thickness of the stamp was shown to affects the pattern transfer and a thin stamp seems to result in better printing quality. This research is not restricted to self-assembly monolayer printing, For applications in which pressure is critical to the quality and yield of printing, the elasticity property of the stamp will be key consideration and this property is directly affected by the thickness of stamp. A uniform, thin layer of stamp is beneficial to other on-going projects in the soft lithography.

Nano-Terra developed their first casting machine (see Figure 6) using aluminum with a 12" master, which demonstrated capability of large area stamp fabrication. In Figure 6, a vacuum chuck at the left hold the backing plate and flips onto the wafer chuck at the right where the wafer sits. PDMS is injected into the gap between backing plate and wafer.

Vacuum Chuck   Wafer Chuck with 12" Wafer
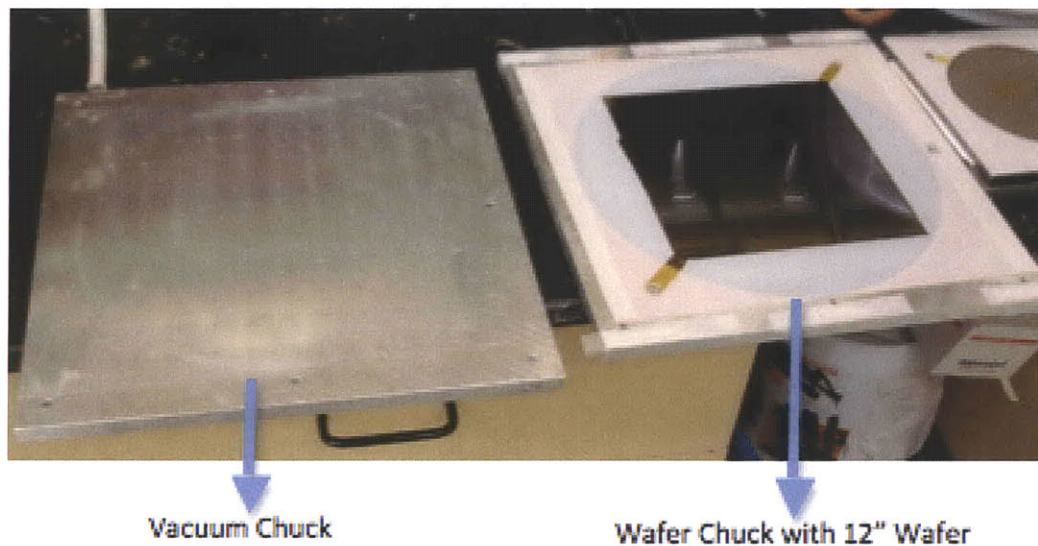
Figure 6: Main Parts of Aluminum Casting Machine for Large Area Stamp, Developed by Nano-Terra LLC.

As shown in Figure 6, this configuration is to have two vacuum chucks : one attaching the master and the other attaching the backing plate. A dam (or reservoir) is placed around the area. These two chucks face each other, and create a space, which is circled by the dam. Liquid PDMS is injected into the area with a syringe.

This pilot stamp fabrication equipment demonstrated consistent quality for use in large size stamp. However it is not designed for interchangeable masters because its mechanism for fixing the master does not allow quick uninstall. Also the space between backing and can't be adjusted easily. Thus it was not able to experiment for manufacturing purpose. Surface finish of the vacuum chuck is rough, which results in uniformed thickness across the stamp.

To resolve these problems identified from this pilot PDMS casting machine, a better material that is capable of ultra-high precision machining is necessary. The Wafer chuck will be modified to add-in alignment capability for maintaining repeatability each time a new master is brought in. Thickness of stamp can be varied by changing the spacing part between wafer and backing plate. This is the topic of Yufei Zhu's thesis [24], detail explanation on stamp fabrication process could be found in his thesis.

2.5 PDMS Peeling Process

The peeling process is a crucial step where we need to wrap a PDM stamp, which initially lies flat on a Silicon wafer, onto the print roller. Thus, it is essential to first successfully peel the PDMS stamp without any tears or distortions. This section studies some of the research that has been done on peeling PDMS off Silicon wafer.

2.5.1 Stress Zones at PDMS Peel-Front

Considerable research has been done on peeling PDMS off a Silicon wafer. However, the upper side of PDMS is not attached to any other surface (like a metal plate), but is open to air. In our project, the topside of PDMS is attached to a steel backing plate. However, some of the findings of the research are indeed useful despite this difference, and are as below.

In general, at the peel front, boundary conditions are different on the two sides of the PDMS stamp; in fact, on one side, the surface of the film has zero shear stress (or very small shear stress, in our case) because it is not attached any surface (or to a different surface), while on the other side, the film adheres to the silicon master and shear stress is imposed on it by the substrate. This configuration creates a singularity around the peel front. This very small and thin zone is characterized by a highly variable stress values. This stress singularity in the normal direction causes the separation of the film at the peel-front.

23

When viewed closely to the peel front, peeling of PDMS could be schematized as in Figure 7:
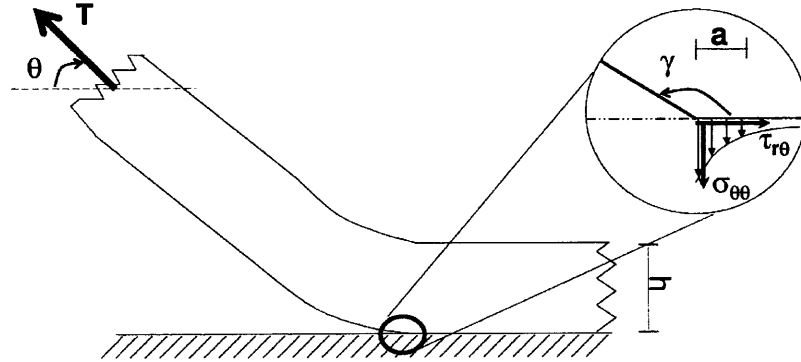
Figure 7: Illustration of Separation at The PDMS-Silicon Wafer Boundary [22].

2.5.2 Initiating Peeling

Generally, to initiate the peeling operation we need apply a force at the peeling front, and as shown in Figure 8, this force can be applied either, A: an upward force on the top surface of the film or B: a force applied at the edge on the bottom surface.

Previous works showed that, the success of either approach depends on how close the applied force is to the vertical plane of the peel-front. Only when the force is applied in the same vertical plane as the edge, the singularity at the edge results in peel-initiation.
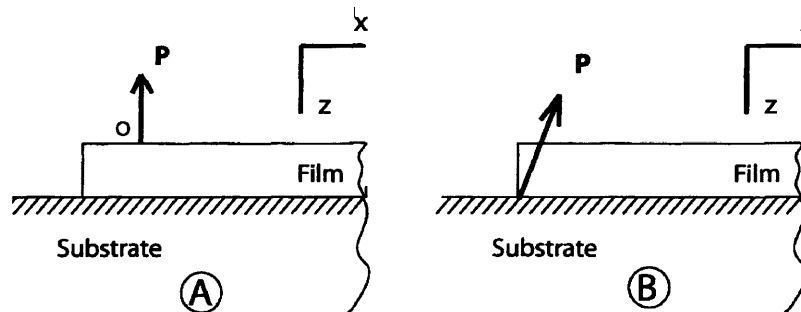
Figure 8: Directions of Peeling Force [22].

24

2.6   PDMS Peeling Process

Since the scope of Nano-Terra 2008 group was limited to monolayer printing using SAM as the conformal printing surface, pressure has low effect on the printing quality. The experiments carried out in 2008 indicate that when printing pressure falls in the range of 15.88kPa to 41.14kPa, or within overall load of 3.5lbs to 26.8lbs, quality of printing is not affected by change of pressure [4]. Because of this character of SAM, the design did not require high precision on the printing area.

Since the machine is designed with three main modules, each module has minimal interaction, thus allowing module upgrade for different purposes. As mentioned before it was built to test the highest achievable throughput using the micron-contact printing technology.

ITEM NO.	DESCRIPTION	QTY.
1	IDLER ROLLER ASSY	1
2	8020 STANDOFF	2
3	IMPRESSION FIXED PLATE	1
4	SHAFT MOUNT	2
5	SHAFT SUPPORT PLATE	1
6	LINEAR BALL BEARING	2
7	LOAD CELL	2
8	PRESSURE PLATE	1
9	LINEAR SHAFT, .750"	2
10	MICROMETER	2
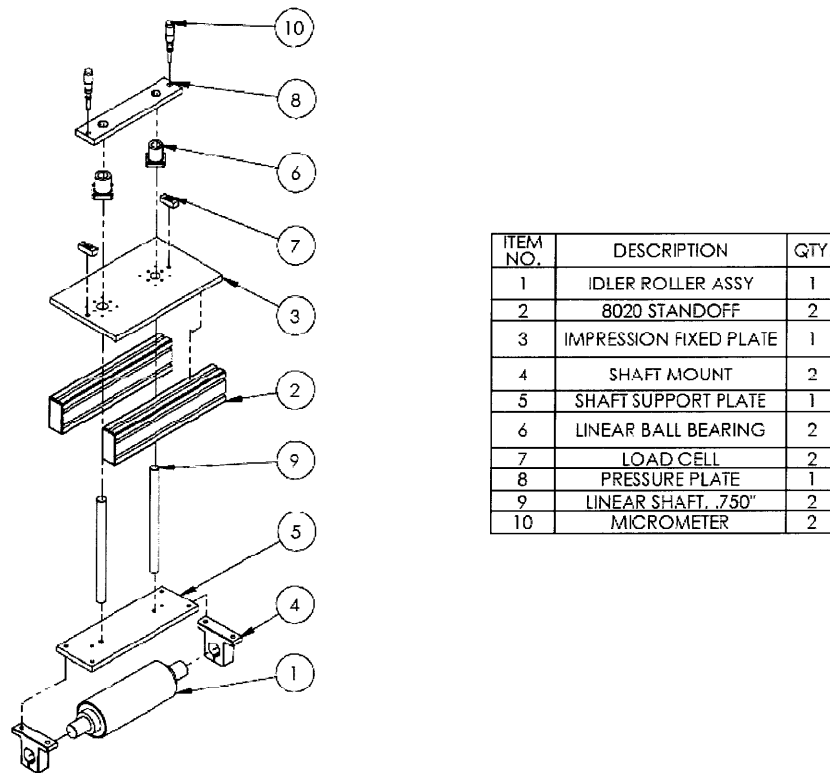
Figure 9: Exploded view of impression Assembly and Bill of Materials [4].

We focused on improving the impression module at the center of this machine (see figure 9 for the explosive view of impression roller system). The Impression Roller Assembly will be replaced (Item #5). The goal of this improvement is to increase the repeatability of web position as well as web path. We also brought pressure sensor into the machine, enabling pressure adjustment for this machine.

All these new improvements are beneficial for future applications other than self-assembly printing. These applications require better pressure control as well as repeatability during printing. We also expected to make the machine more accurate in web handling and the print roller adjustment, both of which are the foundation for multi-layer printing.

In previous project the pressure as printing parameter has been tested. The experiments were carried out by loading impression roller onto a stationary inked printing roller with a strip of substrate in between. Thus the developed patterns after represent the actual contact area between impression roller and printing roller. Because the alignment is not easy to achieve in the print roller, the impression roller and print roller are not parallel and the contact area is tapered, as shown in figure 10.

Figure 10: Image of Different Load From Impression Roller [4].

To investigate the reasons for non-parallel contact, an error budge was carefully studied. As show in table 1, the built-up error of all these components is small compared to error introduced by weight. Under 3.5 pound pressure, the right stripe in figure 12 has top width as 0.09 inch, and bottom width as 0.23 inch[4].

Table 1: List of Parts in Impression Assembly

Item	Description	Qty	Manufacturer	Vendor	Part #	Error
1	MODULE PLATE, PRINT	1	NT-MIT	MD Belanger	P101	0.075mm/40cm
2	SHAFT SUPPORT PLATE	1	NT-MIT	MD Belanger	P114	0.075mm/40cm
3	IMPRESSION FIXED PLATE	1	NT-MIT	MD Belanger	P116	0.075mm/40cm
4	IDLER ROLLER ASSY	1	DFE	DFE	IR3-8-45	N/A
5	LINEAR BEARING ASSY	2	THOMSON	M-C	64825K36	N/A
6	LINEAR SHAFT, .750″	2	THOMSON	M-C	6649K61	0.002″/12″
7	SHAFT MOUNT	2		M-C	6068K27	N/A
8	8020 STAND OFF	2		8020		N/A

2.7 Multi-Layer Printing

After the successful demonstration of high throughput and good yield in one-layer printing using R2R machine, our background knowledge is sufficient to start the research in micro-contact printing's capability of multi-layer printing. This is an important step towards the actual application in manufacturing because micro-contact printing is no longer limited to printing of photo-resistive material as the ink. Further applications require multiple layers to overlap to achieve complex function. The units under consideration include diodes and transistors with at least 3 layers.

An important specification introduced in multi-layer printing is accuracy in relative layer position or registration. We are expecting to achieve registration with the roll-to-roll structure, because of the high throughput. However most literature discusses methods to align surface to surface, including the alignment between mask and wafer in semiconductor industry, or dip and substrate in inkjet printing, while few have mentioned alignment issue between round subject and flat substrate. Thus references for designing machine capable of multi-layer printing will be mainly from color printing industry.

It is common practice to start building high precision system based on an open-loop structure and to add-in close loop component to increase the accuracy. An open-loop structure is simple because micro-contact printing requires only two motions: linear motion of substrate and rotational motion of the print roller. Since roll-to-roll machines are widely used in printing industry, it is beneficial to learn how the feedback systems work. We will use gravure printing to demonstrate how the printing industry achieves this registration. Figure 11 shows a typical gravure-printing machine.

Figure 11: Gravure Printing Machine.

Gravure is widely used in high quality printing. Because human eyes are not sensitive to features less than 40 micron wide, the feedback system for gravure machines usually sets the accuracy at 100 micron or less. Errors in two key directions have been compensated. One is the direction of substrate motion during printing, or the "path"; the other is the direction perpendicular to the path on substrate plate. The latter is easy to adjust by moving roller along its axis; the error in path is sensed and compensated using sleeve displacement between the roller and the sleeve (see Figure 12).
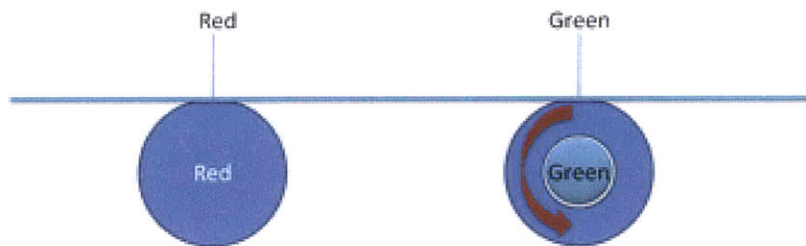
Figure 12: Actuation Method For Adjusting The Relative Distance Between Print Nips on The Substrate.

In Gravure printing, marks are printed with a distance of 20mm, and individual roller prints each color mark. Sensors are used to check the distance between marks to determine the relative position between different colors on substrate. The sensor system is shown in Figure 13. The signal from sensors are received only when designated color are about to arrive. Once an error is detected, the controller will send out signals to the roller whose color is offset from its desired position, and the sleeve on the roller will rotate to compensate for this error.
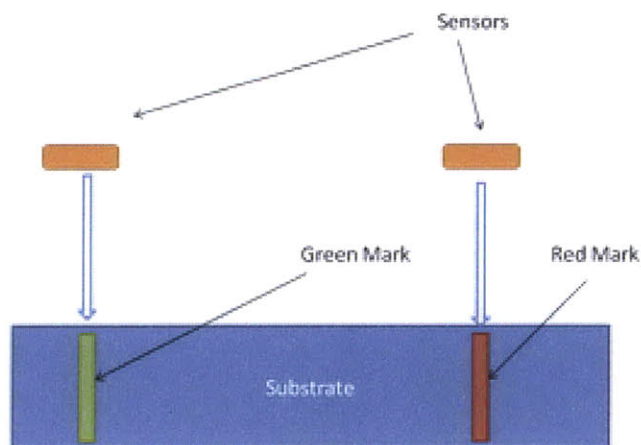
Figure 13: Simplified Sensing Method For Detecting The Relative Position Between Two Layers of Print in Gravure Printing.

Assume both red and green rollers are rolling at the same speed, the green and red mark on the substrate will have a constant distance of 20mm, and signals from both sensors will reach controller at the same time. If, however the green roller is one step behind compared to the red roller, the green mark will shift back at some distance, and a signal from the green sensor will lag from the red signal. The controller will determine the amount of offset from the time of this lag and control the sleeve on green roller to shift one step ahead.

2.8 Optical Methodology System Review

One of the objectives of the project is to fabricate the stamp within the variance of ±4μm, which means high precision measurement tools has to be employed. Currently, there are various kinds measurement sensors that can achieve very high accuracy and resolution, but they also have specifications that match some specific needs. In this section, laser triangulation sensors, interferometers, fiber optic sensors and con-focal microscopy are reviewed as our potential choice of measurement sensors.

2.8.1 Laser Triangulation Sensors

Triangulation measurement is an old but very useful method to measure distance. Laser sensor is a powerful tool, using triangulation measurement, to measure either long-distance or short-distance with high accuracy. However, the long distance measurement may not provide very high resolution. Laser sensor projects a spot of light onto the target and receives the reflected light with photo detector through an optical lens. A typical laser triangulation system is shown in Figure 14 below.
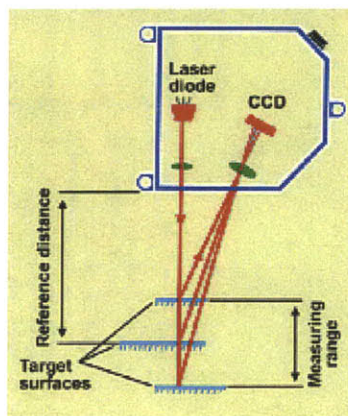
Figure 14: Principal of Laser Triangulation Sensor[14].

29

From the Figure 14, we could see that the relative position of laser diode, lens, photo detector and the position of reflected light from the target on the photo detector determine the distance of the target. If the target changes it position, the reflected the light changes its position on photo detector as well. Through linearization and additional digital or analogue signal processing, the detector could provide an output signal proportional to the position of the target. The ambient light has little effect on reading, because the signal is proportional to the center of intensity of focused image [14].

The most important part of laser sensor is the photo detector, which could be photo diode, position sensitive device (PSD), charge coupled device (CCD), Complementary metal–oxide–semiconductor (CMOS), etc. Different photo detector requires different signal processing method.

The following summary of general laser triangulation sensors' characteristics is built upon the works done by Alexander H. Slocum in his book named *Precision Machine Design* [15], updated with recent industry standards. Note that the manufacturers are always advancing the state-of-art, so this summary is generalization only.

- **Size:** Typically 30x50x70mm.
- **Cost:** Depends on the resolution. Normally, 1 μ resolution laser sensor cost $4000.
- **Measurement Range (span):** 3 - 1300mm.
- **Accuracy (linearity):** 0.03% of Span, 500 Hz, to white target (85% diffuse reflectance).
- **Repeatability:** Depends on the repeatability of the surface finish.
- **Resolution:** on the order of 0.005% of full-scale range, could achieve as high as 0.1μm.
- **Laser spot size:** 30-300μm.
- **Environment Effect on Accuracy:** On the order of $0.01\%/^{0}C$ of full-scale range from the nominal $20^{0}C$ operating temperature.
- **Power:** 15 – 24 Volts DC, 120 – 200 mA draw with 350 mA surge at power-up.
- **Allowable Operating Environment:** Keep optical windows clean for best performance. System typically operate from 0 to $40\,^{0}C$.

2.8.2   Interferometer Sensors

Various kinds of interferometers are in use today. Michelson interferometer has the most common configuration for optical Interferometry and was invented by

Albert Abraham Michelson. A typical and simplified interferometer system is shown schematically in Figure 15.
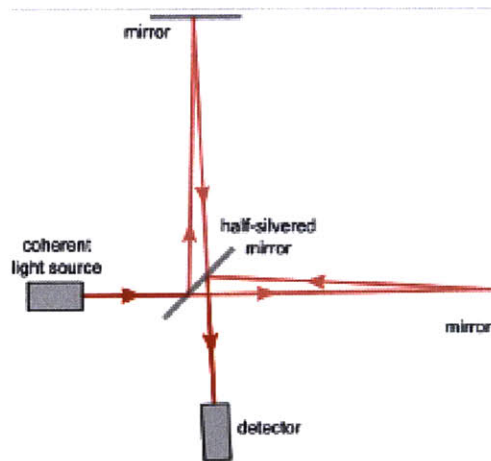
Figure 15: Principal of Interferometer System[15].

According to Figure 15, a continuous light source was spitted into two paths: one bounces back from the semi-transparent mirror, and then reflects back from the mirror on the top, goes through the semi-transparent mirror, to the detector. The other one goes through the semi-transparent mirror, bounces back from the mirror at right, and then reflects back by the same semi-transparent mirror and goes into the detector. Difference in path may result from the length difference or different materials, which cause alternating pattern on the detector. If no difference of materials involved in the interference, the distance could be measured through.

The following summary of general laser triangulation sensors' characteristics is built upon the works done by Alexander H. Slocum in his book named *Precision Machine Design*[15], updated with recent industry standards. Note that the manufacturers are always advancing the state-of-art, so this summary is generalization only. It is also extremely important to stress that the accuracy of measurement is highly depended to the manner of how the optics are mounted and how the environment are controlled.

- **Size**: Laser head, 130x180x530mm.
- **Cost**: About $9000 for laser head and electronics boxes for up to 4 axes of measurement.
- **Measurement Range (span)**: up to 30m[16].

- o **Accuracy:** In a vacuum, if perfectly aligned, the accuracy can be on the order of half (worse) the resolution. As for non-vacuum conditions, the environment significantly impacts the accuracy of measurement.
- o **Repeatability**: Depends on the stability of the environment and the laser head.
- o **Resolution**: Depends on optic used and can be achieved as high as $\lambda/4096$. Higher resolution could be achieved through better optics and phase measurement technique involved.
- o **Environment Effect on Accuracy:** About $1\mu m/m/^0C$ Air turbulence and thermal expansion of optics, mounts and the machine itself [16].
- o **Power**: 12 V, 200 mA (PICO M8 con.).
- o **Allowable Operating Environment:** Since the interferometer is sensitive to the environment, ideally, it should be used in a vacuum, or in air of 20^0C with no gradients.

2.8.3 Fiber Optic Sensors

Optical fibers are glass or plastic fibers that transmit light using the property of total internal reflection and the fiber act as waveguide. Figure 16 demonstrates the total internal reflection of a laser inside the optical fiber.
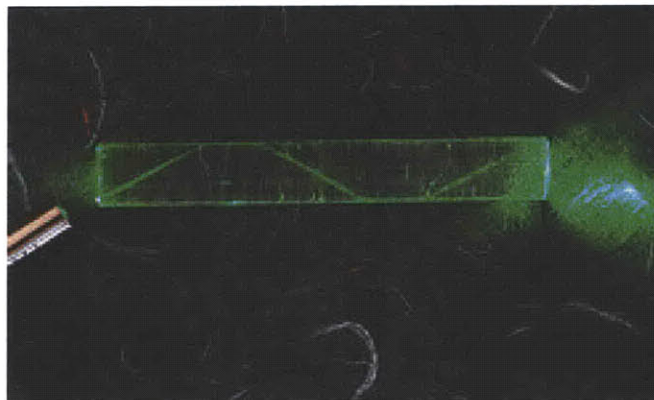
Figure 16: Total Internal Reflection inside Optical Fiber[15]

The key elements for fiber optic sensor are two sets of flexible probes: one is for transmitting and the other is for receiving. Two probes are jacketed into one to measure the distance. There are basically three kinds of probes configurations: Hemisphere, Random and concentric, as shown in Figure 17. Active diameter of probes could be as small as 0.177mm, making them ideally suited to small target measurement [17].

Random
(R)

CONCENTRIC
TRANSMIT
INSIDE
(CTI)

• Receiving Fiber
○ Transmitting Fiber

Hemispherical
(H)
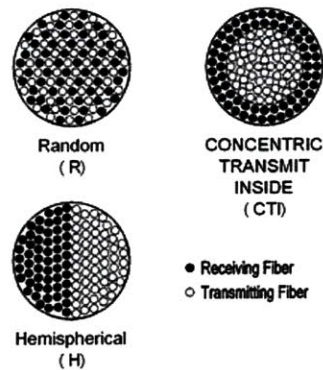
Figure 17: Fiber Optic Probe Configuration [17].

The distance of an object can be determined based on the intensity of reflected light that is sensed by two transmitting and receiving fiber probes [18]. The response curve is shown in Figure 18, and the intensity of reflected light is converted to voltage output. Optic Fibers are not sensitive to electromagnetic interference and typically very light [16].
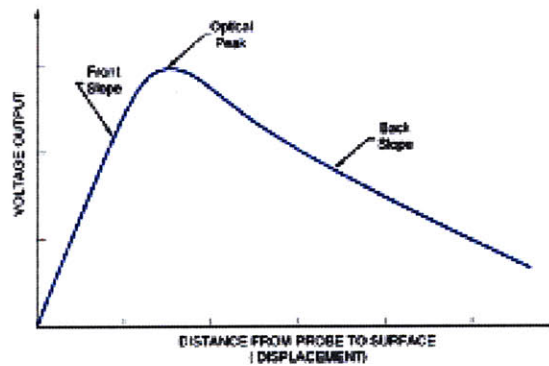
Figure 18: Fiber Optic Probe Response Curve [17].

The following summary of general laser triangulation sensors' characteristics is built upon the works done by Alexander H. Slocum in his book named *Precision Machine Design [15]*, updated with recent industry standards. Note that the manufacturers are always advancing the state-of-art, so this summary is generalization only.

- o **Size**: cable diameter could be 1mm or even smaller.
- o **Cost**: Depends on the type of sensor, $100-$1000.

- o **Measurement Range (span)**: a few millimeters for small displacement (<10mm).
- o **Accuracy:** 0.1% of full range.
- o **Repeatability**: Depends on environment conditions.
- o **Resolution**: Can achieve very high resolution if the sensor held very close to the target, like 0.01μm resolution with the range of 0.1mm.
- o **Environment Effect on Accuracy**: very sensitive to environment, like dirt on the sensor will degrade the performance.
- o **Allowable Operating Environment:** Since the interferometer is sensitive to the environment, the sensing surface must be kept very clean. Individual probes should be kept away from moisture, or they will eventually erode to the point of failure.

2.8.4 Con-Focal Laser Scanning Microscopy

Con-focal laser scanning microscopy (CLSM or LSCM) is a technique that could capture very sharp images at selected height[23]. A very important feature of con-focal microscopy is that it could obtain in-focus images from various depths. Because of its high resolution on depth measurement, the con-focal microscopy could be applied to measure the flatness of object within the limitation of the measurement tool.

In con-focal laser scanning microscopy, a coherent light source projects a beam of laser, which goes through the beam splitter and focused on the target via lens. Scattered and reflected laser light, together with the illumination light, were re-collected by the lens and then focus on the detector via the reflection of the same beam splitter. The aperture of detector blocks the light that is not from the focal point and hence leads to a sharper image comparing to conventional microscopy (See Figure 19).
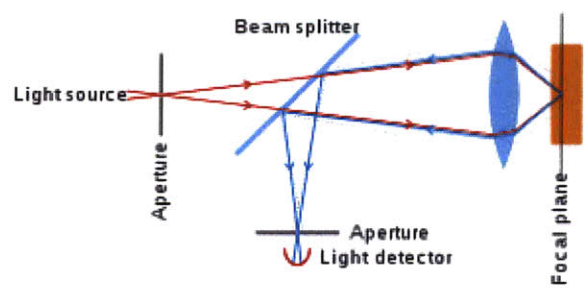
Figure 19: Principal of Con-Focal Microscopy[23].

Adjusting the position of lens could allow light detector capture the sharpest image of the targeted area. Most of current con-focal measurement systems could

accomplish supplementary measurement by using CCD to detect the target and measure its position.

In this project we are using Nikon VERITAS VM250 as our main metrology to test the surface flatness through measuring the depth of the sample points. The following is the summary of general characteristics of Nikon VERITAS product series.

- o **Size**: Main body - 565 x 690 x 740 mm (minimum height), 72kg; Controller - 145 x 400 x 390 mm, 13kg.
- o **Cost:** Depends on the type the precision and measurement range, more than $10,000.
- o **Measurement Range (span)**: could achieve 50mm.
- o **Accuracy:** could achieve 1 μm.
- o **Repeatability**: rely on xyz moving stages.
- o **Resolution**: Can achieve 0.1μm.
- o **Power:** AC100-240V±10%, 50/60Hz.
- o **Environment Effect on Accuracy**: within allowable operating environment, the accuracy can be well maintained.
- o **Allowable Operating Environment:** Temperature - 10ºC to 35ºC; Humidity - 70% or less.

CHAPTER 3 - Methodology

3.1 Stamp Casting Machine

Before processing the casting machine compatible with 12" master, we started with a 6" casting machine to see the capability of the design and building material (316 Stainless Steel). The design allows both 150mm wafer and 200mm wafer to be used in the same configuration. The stamp-casting machine will be capable of alignment for different masters. We use pins to locate wafer. In order to hold tight the wafer during pouring PDMS, grooves are designed for vacuum capability and wafer will be held using vacuum after aligning (see Figure 20). Because no glue or tape will be used in the process, wafer will be easily replaced once the vacuum has been turned off.
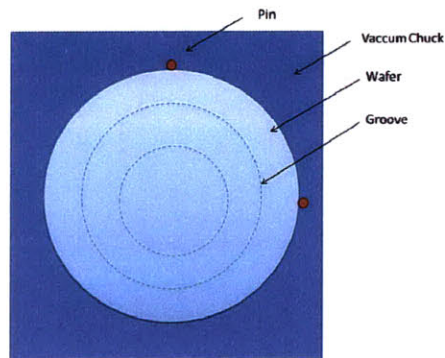
Figure 20: Structure for Wafer Chuck.

A single piece of Teflon with a rectangular opening inside will attach to master as the dam for holding PDMS within the area, this Teflon will also act as spacer between master and backing plate (see Figure 21). Shape and the thickness of the stamp on the backing plate are determined by this Teflon.
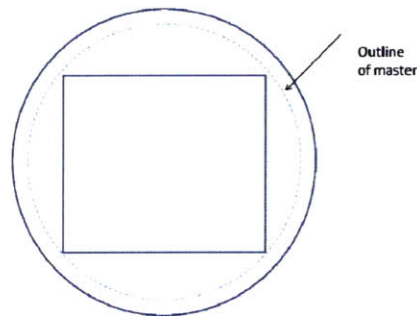
Figure 21: Teflon Spacer.

The area for containing PDMS is confined by:

- o Wafer on the top for transferring pattern.
- o Thin stainless steel sheet (backing plate) sitting at the bottom as the backing for PDMS.
- o Dam between wafer and backing plate for holding the PDMS.

Repeatability is the critical design specification. Under this configuration, making a single big stamp will require many identical steps, and each step will result in a small area of finished stamp. Variables to be considered are:

- o Distance between master and backing plate (all attached to the chuck).
- o Displacement between master and backing plate.
- o Uniformity of the stamp.

All these variables can be decomposed in 6 dimensions: 3 linear and 3 rotational. A sidebar is used to align both chucks, as shown in Figure 22. The backing plate chuck (referred as SS Vacuum Chuck) is fixed to the side bar, while the adjunction of wafer chuck and sidebar leaves some clearance for adjusting. Minor adjustment is done by using screws to locate wafer chuck in both X and Y directions. The Z direction, also determines the height for stamp, is fixed by the thickness of dam.

Sidebar

Wafer Chuck

Stainless Steel Chuck
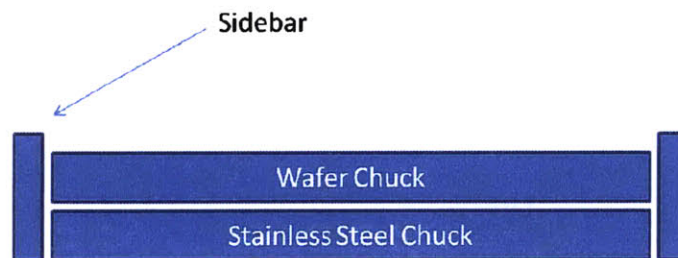
Figure 22: Sidebars Used to Align Both Chucks.

Because the fabrication of stamp from PDMS is done in a low-pressure environment, the chucks with dam inside will be clamped together with strong force to ensure no air leaks in. Traditional C-clamp does not fit here because point contact will create distortion. Our approach needs to distribute the force as uniformly as possible. A clamping bar connected to sidebar by screw is used to provide clamping force. Small precision springs will be inserted between the clamping bar and wafer chuck to apply equal force.

3.2 Peeling and Wrapping the Stamp on the Print Roller

The R2R machine that was built by MIT'08 group proved that the R2R technique is feasible with micro-contact printing technology, but experiments showed that the printed images were affected by many distortions. The current way to wrap the PDMS stamp on the print roller is performed manually using a seam on the cylinder. The challenges in the manual wrapping process using a seam demand the intervention of a skilled operator, making the process both time-consuming and labor-intensive. Also, even if all the operations will be performed in the correct way is not possible to guarantee the 5 microns alignment as required.

Therefore, the first goal of the project consists of improving the printing quality, designing a way to peel and wrap the stamp that will respect the following aspects:

- o Maintain alignment.
- o Fast replacement .

3.2.1 Gripping the Film for Peeling

The setup of the print roller before wrapping process is shown in Figure 23. This setup comes after flat stamp fabrication process: dissembling the vacuum chuck from the fabrication device and placing the print roller at the edge of the backing plate.
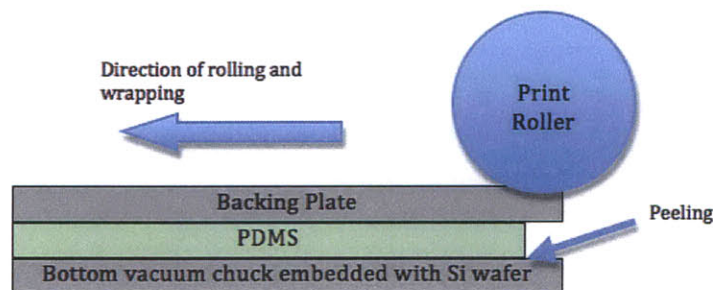
Figure 23: Illustration of Pint Roller Setup before Wrapping.

Any device that grips the backing plate for peeling off the stamp must accomplish three steps in the peeling process:

1. Initiate the peel.
2. Separate the film from the wafer.
3. Transport the peeled film away.

38

Unfortunately, the first and second stages are complicated by the inherent physics of peeling that we discussed in the literature review in the previous chapter. Let us begin by looking at the initiation of separation. This is a difficult step because the PDMS film adheres over the entire area of the substrate, leaving no 'lip' to hold the film or to start the separation. When an operator introduces a lip by inserting a razor, she must be careful not to scrape the film or inadvertently cut through it. Once she initiates separation, the operator may pull the film at point-contacts, which may cause excessive stresses and risk tearing around the contacts. If the film is adhered well to the substrate, she may need to pull hard on the PDMS film, which could also cause tearing.

Therefore, it is necessary to design a system that is able to grab and wrap at the same time the PDMS stamp that performs the following:

1. Grab the PDMS stamp without causing breaks or plastic deformations
2. Keep peeling the PDMS stamp applying a force with constant intensity, constant direction, and with a uniform distribution.
3. Wrap the PDMS stamp on the roller without loosing alignment and without causing relative motion between cylinder and backing plate.

Keeping in mind the above requirements, we designed and analyzed concepts for peeling and wrapping the PDMS onto the backing plate. These concepts have been summarized below. It should be noted that, based on the results of the MIT '08 project, it is evident that this step of peeling and wrapping with precision and alignment is the most crucial step, in that it has a direct bearing on the printing quality.

3.2.2 Methods to Generate Adhesive Force between Backing Plate and Print Roller

Through the industrial investigation, we summarized the concepts, which are available on the market, to search for optimal solution the generate adhesive force between backing plate and the print roller:

1. Electro magnet cylinder.
It has ability to switch on and off the magnetic force of attraction, thus enabling better manual control over the pre-alignment of the print roller positioning with respect to backing plate. However, the electro magnet cylinder requires additional electrical components and needs complex additions or modifications to print roller.

2. Permanent magnetic cylinder.

It could provide strong magnetic force, even if rare earth magnets used, which is easily available. On the other hand, a permanent magnetic cannot switch off magnetic force. Also to machine a cylinder with permanent magnetic force is expensive and it is difficult to obtain precision in diameter.

3. Cylinder with vacuum force.

The vacuum holes along the cylinder could provide uniformly distributed attraction force along surface of cylinder. The vacuum cylinder is adaptable from existing commercial vacuum rolls. Nevertheless, the vacuum cylinder requires additional vacuum pump and vacuum control. And backing plate will have to cover entire vacuum-surface of cylinder; otherwise leakage of vacuum could be an issue.

4. Cylinder with double sided adhesive tape on the surface.

Attaching the double-sided tape onto the surface of the cylinder could also provide strong adhesive force and such design is obviously simple and easy.
The disadvantage of this method is that the double-side tape Introduce another layer between the print roller and the backing plate which another source of variation on the roundness of the roller. In addition, it is difficult to correct errors of misalignment of backing plate with cylinder. Furthermore, cleaning cylinder for stamp replacement would be very difficult.

Chosen Method: Through analyzing above those possible solutions of the print roller, we finally decided to use stainless steel cylinder with a series of permanent magnets embedded into the cylinder. This kind of cylinder is a well-established design for use in the die-cutting and embossing industry, hence easily available. Also, this design satisfies all the precision and accuracy requirements with respect to the diameter, total run out, and straightness of the cylinder.

3.2.3 Methods to Wrap Backing Plate without Losing Alignment

1. Slot in print roller, clamp to grab backing plate

Clamp refers to an L shaped projection that would slip between the backing plate and the Si wafer. This would enable a positive grabbing or locking of the backing plate with the print roller, it requires pre-alignment before clamping.

2. Slot in print roller, bent edge of backing plate

This would be similar to using a clamp, except that the backing plate would be bent, and would stick out, enabling one to insert the bent edge into a slot in the print roller, again accomplishing a positive locking arrangement. But the relative

position of the edge of backing plate and the slot has to be very accurate in order to maintain the alignment.

3. Pins in roller, holes in backing plate

This design consists of two (or more) pins inserted using threaded holes in the body of the cylinder. Corresponding holes would be drilled or machined in the backing plate. The height of the pins sticking out of the cylinder would be less than the thickness of the PDMS (less than 500 microns). This would prevent damage to the wafer during peeling and to the substrate during printing. Also the pins and holes could provide enough assembly constrains to guarantee desired alignment.

Chosen Method: Pins in roller, and holes in backing plate. This was found to be the simplest, easiest to adapt, and the most precise design.

3.2.4 Analysis of Fixture System

A fixture system that helps to guide the movement of the print roller during the wrapping was designed, as shown in Figure 24. The fixture would serve two purposes:

1. Pre align cylinder with backing plate.
2. Maintain alignment during wrapping of the backing plate on the cylinder.

However, the fixture system over constrains the cylinder-backing plate during wrapping. This is because, the force of adhesion between the cylinder and backing plate already achieves alignment between the two. Hence, if the fixtures try to achieve a slightly different alignment, it would create distortions and twisting forces in the backing plate, which would lead to detrimental effects on the stamp, and induce unwanted stresses in the stamp.
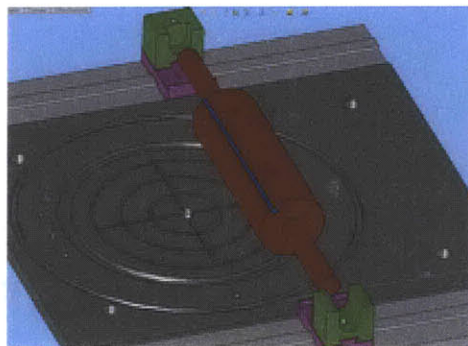
Figure 24: Illustration of The Proposed Fixture System.

Upon conducting experiments with a prototype Aluminum cylinder, with pins, and holes on backing plate, and conducting error analysis for the same, it was decided that pin-holes are the best way to minimize alignment errors between the backing plate and print roller. Thus, the fixture system was not used.

3.3 Precision Measurement Method

The initial goals of this project were to fabricate a stamp with uniform thickness, wrap the stamp onto the roller with uniform roundness and demonstrate multi-layer printing. In order to answer the questions such as how thick the stamp is, how flat the stamp is, how good the quality of multi-layer printing is and etc., a thorough measurement method needed to be develop to precisely and correctly answer those questions. Meanwhile, multi-layer printing requires upgrading the accuracy of alignment of the current R2R system, so a systematic measurement is also desired to demonstrate the improvement of alignment in accuracy.

3.3.1 Flatness and Roundness Measurement

In the stamp fabrication and wrapping process, the ultimate goal is to make sure that the diameter of print roller has the variance of ±4μm, and the print roller here means the assembly of the central shaft, sleeve, and the backing plate with the stamp. All the potential variance could be broken down into following categories:

- o Flatness measurement

  - Flatness of stainless steel.
  - Flatness of the PDMS stamp.
  - Uniform thickness of attached PDMS on stainless steel.
  - Flatness of devices that are used to fabricate the stamp.

- o Roundness measurement

  - Roundness of print roller.
  - Roundness of central shaft.
  - Eccentricity of the motion of the driver motor.

Due to the specific characteristic of PDMS and the overall process, the measurement device should obtain following requirements:

- Non-contact measurement.
- High resolution, targeting on 1µm.
- Sufficient range (>1mm).
- Affordable.

At first, Laser triangulation sensor was the first choice, which is perfect aligned with all above requirements. Corresponding fixtures and frames were developed for the flatness and roundness testing, as illustrated in Figure 25. Basically, the laser sensor sits on the micrometer head for the fine adjustment and the micrometer head is mounted onto the frame to test either flat or round surface.

Flatness measurement   Roundness measurement
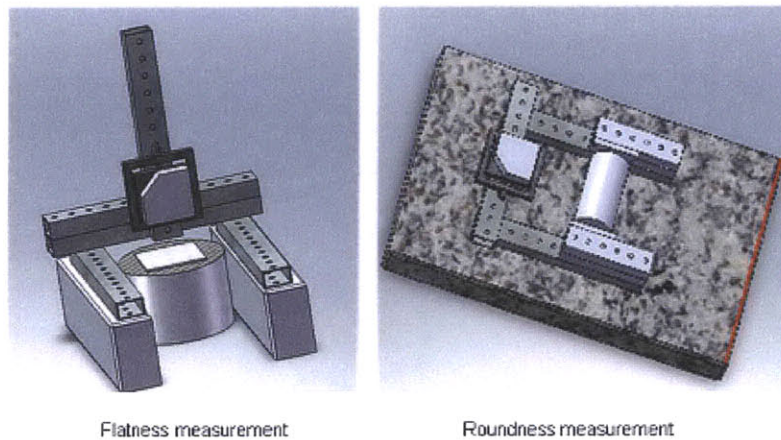
Figure 25: Fixtures for Flatness and Roundness Measurement.

However, the chosen laser sensor cost more than $4000 and could only be used for this project in the view of Nano Terra LLC, which is not cost effective for the company in sake of the future application. Therefore, we plan to use the available CNC Video Measuring Systems (Nikon VERITAS VM 250) that could measure the height of the surface by using con-focal technology. (The machine is shown in Figure 26).
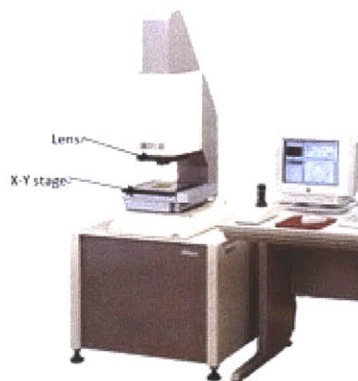
Figure 26: VERITAS VM 250.

To measure the flatness using Veritas, the object should be placed onto the x-y stage and measure the height of sample points on the surface of the object. Since the x-y stage could move alone x and y axis in a perfect flat surface, it help to keep away from the disturbance introduced by the measurement equipment.

Roundness of the print roller is targeted because of its critical impact towards the printing quality. Although the roundness of print roller is very forgiving in self-assembly materials and the impression roller, which contacts the print roller during the printing process, could tolerate the variance of the roundness, the high roundness print roller is still desired in the view of future development. Because, if using some other materials that do not have self-assembly characteristics or very little pressure could be applied onto the print roller, a perfect roundness print roller is highly important to the final print quality.

In actual measurement, there is a problem with the roundness test due to the optical properties of PDMS. PDMS is an elastic transparent material that does not allow the laser sensor or the dial indicator to precisely measure the roundness variance. A few solutions could be applied to solve this issue: An interferometer is not limited by such kind of materials but it is too expensive for this project, or the stamp could be coated with metal powder and then use laser sensor to measure the distance, but this method will cause the damage of the stamp. Finally, the roundness of the printer roller could be indirectly indicated by the accumulate effect of the roundness of the print roller with the stainless steel sheet and the flatness of the stamp. The stamp is seamless attached to the stainless steel sheet; therefore, we assume the variance caused by the attachment is zero.

In the roundness test, since we are only interested in how round the print roller is when it is rolling for printing, and we are trying to compare the performance of different two wrapping systems, the measurement is taken separately in the two systems (i.e. that previous R2R system and updated R2R system detailed below) while simulating a real printing process. The final roundness information of the print roller is the aggregated result of the motor shaft eccentricity, motion transition quality of the connected bearings, roundness of the central shaft, roundness of the sleeve, variance caused by assembling the sleeve on the shaft, firmness of the attachment between the stainless steel sheet and the sleeve, and the flatness of the stamp. A dial indicator was used to make this measurement and Figure 27 illustrates the general idea of the measurement settings.
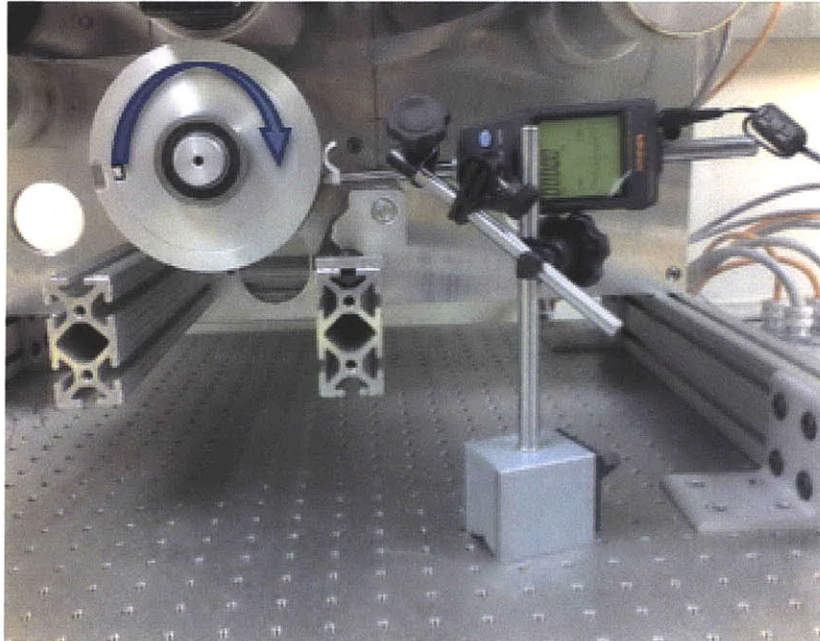
Figure 27: Measurement Setting for Roundness Measurement.

With each rotation of the print roller, 16 sample points of were collected at 3 positions along the roller (Front, Middle and Back), which means 16x3 sample points are collected for roundness analysis.

3.3.2 Distortion Measurement

After the features are successfully transferred from the stamp to the substrate (gold coated PET is the substrate used in this project), one of the most important quality indicators is the distortion of pixel on the substrate. The distortion is caused by several reasons:

1. The distortion of the flat stamp during the fabrication process.
2. The distortion caused by wrapping the stamp onto the print roller.
3. The tension of the substrate causing stretch of the feature.
4. The print pressure slightly deforms the features on the stamp.
5. Other noises.

All above sources of the distortion had been carefully analyzed in the thesis of *Analysis of the Capabilities of Continuous High-Speed Micro-contact Printing*[20] by Kanika Khanna. Based on her study, the wrapping process contributes the most to the final distortion.

The overall pattern printed comprises two types of pixel patterns, rectangular and triangular, as shown in Figs 26 and 27. The array of both of these pixel patterns is shown in Figure 28, where each pattern is printed on a 1.5mmx1.5mm square[20].

Figure 28: The Shape of Rectangular- like Pixel.
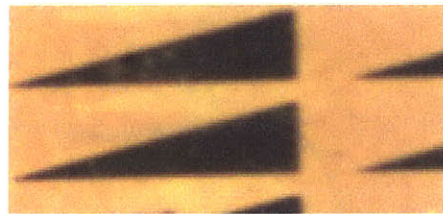
Figure 29: The Shape of Triangular Pixel.
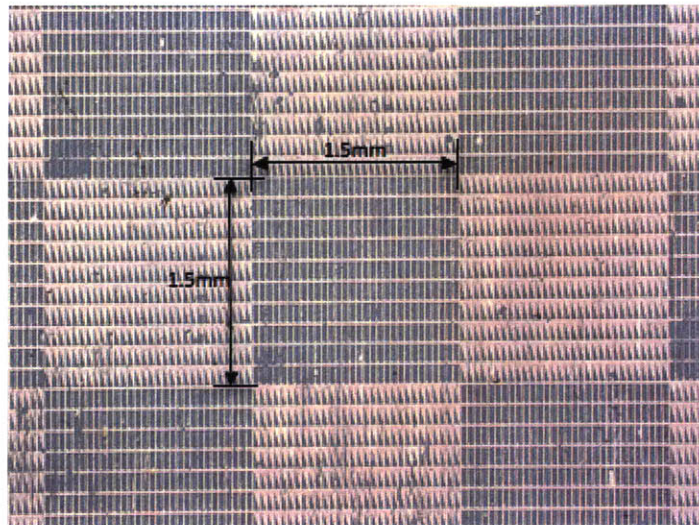
Figure 30: The Array of Two Kinds of Pixels.

As mentioned before, the wrapping process causes distortion of the stainless steel sheet, which is used to hold the stamp in the printing process. The distortion of the stainless steel sheet leads to distortion of stamp, and hence the distortion of pixels. Figure 31 demonstrates the distortion of pixel in a simply way. The black dashed rectangle is the standard shape of the pixel on the substrate and the blue

solid rectangle is the distorted printed pixel. In Figure 31, X and Y indicate the horizontal and vertical dimension of the standard pixel; X' and Y' indicate the corresponding dimension of printed pixel. It is important to note that the shape of distortion varies based on multiple reasons. To indicate the distortion, we will just simply use Y'/Y and X'/X as the distortion rate to identify the distortion over the Y and X axis.
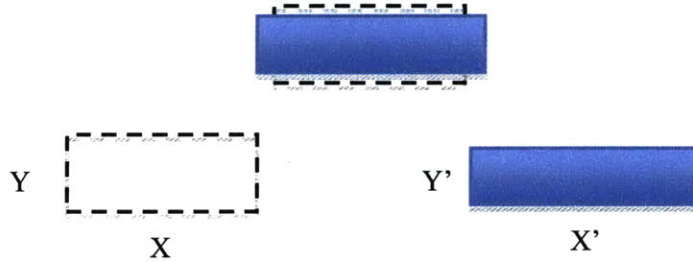
Figure 31: Demonstration of the Distortion.

In order to make things easy, the distortion measurement is only taken on the rectangular-like pixels shown in Figure 28, which is statistically representative to the overall distortion. For those rectangular-like pixels, their standard dimension is 130μmx40μm as shown in Figure 32.

It is important to distinguish pixel distortion from pattern distortion. In this work we concentrate on distortions of at the pixel level, and are not concerned with overall pattern distortion caused by web movement or a non-parallel stamp on the roll. The stamp is made from a 300mm wafer, and the actual size of the square stamp is 200mmx200mm. This area is evenly divided into 5x5 cells with each cell being 40mmx40mm. Within each cell, 5 pixels are randomly picked to measure, and averages to minimize the measurement error. This average is used to represent the dimension of the pixels in this area.
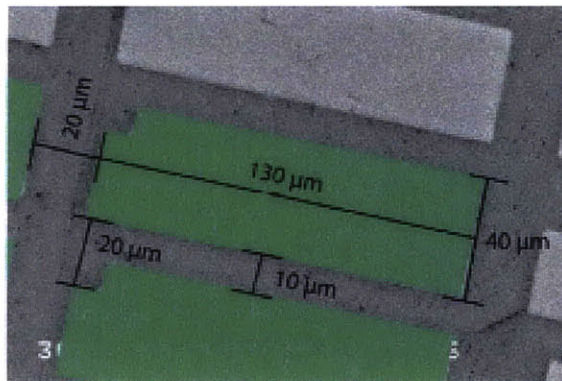
Figure 32: Pixel Dimensions[20].

3.3.3 Measurement of the Accuracy of the Alignment

The scope of the multi-layer printing in this project is to use the stamp to print twice on the same substrate without loosing alignment. Therefore the accuracy of the alignment could be measured by indicating how well the overlap of two printed features, shown in Figure 33. In current stage, only x and y displacement are concerned. The angular misalignment is not included in the measurement due to the time constrain.
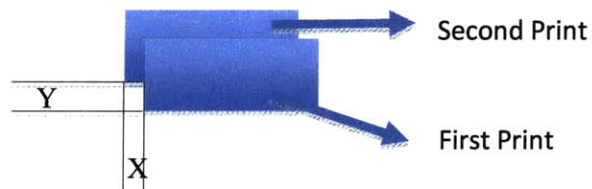
Figure 33: Displacement of Two Printed Layers.

Same to the measurement of distortion, 5x5 matrix divided the 200mmx200mm printed area into 25 squares. Take the average of 4 measurement within each square for the x and y displacement.

CHAPTER 4 – Necessity of a High Precision Positioning System

4.1 Introduction

In its current state, microcontact printing is limited to lab scale testing with low production rates. In 2007, a group of MIT engineering students demonstrated that microcontact printing was feasible in a roll-to-roll continuous format. Their machine demonstrated the feasibility of much higher production rates than the state of the art machine and made observations regarding key parameters necessary for a quality end product. In 2008, another group of MIT engineering students expanded their knowledge gained from the previous group, further applied technologies borrowed from traditional roll-to-roll processes, and at the same time created new tools especially tailored to microcontact printing."[4].

In particular, the team 2008 developed a prototype printing machine and continuous etching machine. Additional hardware was also designed and built in order to further experiment with this new technology. The prototype built last year showed that roll-to-roll microcontact printing can produce high quality results over large areas at rates up to 400 feet per minute and possibly beyond. The printing quality achieved by this machine was within 66μm[20].

As stated in Chapter 1, the current goals are to improve the printing quality and to conduct experiments on the multilayer printing process. Therefore, as a first step, an accurate analysis of the current system was performed in order to identify the critical components to improve. After the first general analysis, studies were focused on the printing module.

4.2 Analysis of the Current Printing Module

The current printing module is the most critical assembly of the machine. It encompasses all of the most important functions: stamp mounting, printing speed, printing load, substrate-stamp wrap angle, and inking. The printing module system consists of two subassemblies, an exploded view of which is shown in Figure 34:

1. The print roller subassembly includes the main stepper-motor-powered roller that drives the stamp against the substrate. A PDMS covered roller below the stamp roller can be lifted and engaged to ink the stamp. The accuracy and repeatability of this assembly has a significant effect on the

printing quality as all the most critical processes occur at this station. Stamp mounting flatness, shaft eccentricity, vibration, and a number of other factors contribute greatly to the performance of the machine.

2. The impression roller assembly consists of a stage that the impression roller rides on. The impression roller is a foam-covered roller that applies pressure to the substrate as it rides over the Stamp Roller. A pair of load cells is used to measure the force applied.
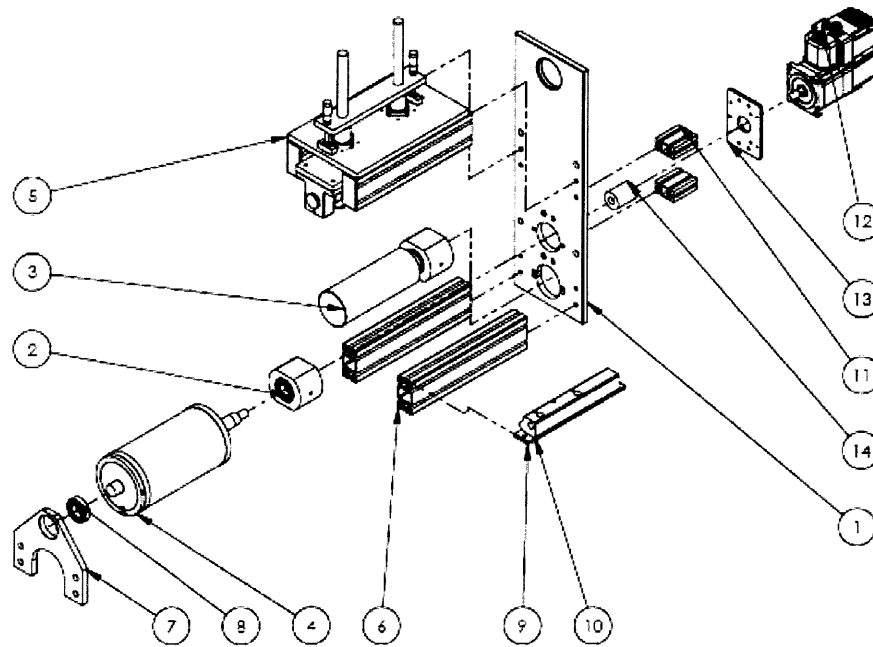
ITEM NO.	DESCRIPTION	QTY.
1	MODULE PLATE, PRINT	1
2	BEARING BLOCK ASSY	2
3	INKING ROLLER	1
4	STAMP ROLLER ASSY	1
5	IMPRESSION ROLLER ASSY	1
6	8020 STANDOFF	2
7	BEARING PLATE, PRINT	1
8	BALL BEARING, 1" ID 2" OD	1
9	AIR KNIFE MTG PLATE	1
10	AIR KNIFE	1
11	MOTOR STANDOFF	2
12	STEPPER MOTOR NEMA34	1
13	MOTOR MOUNT PLATE	1
14	COUPLING	1

Figure 34: An Exploded View of the Printing Module[4].

The current printing module is characterized by:

- An accurate and precise printing force.
- A precision tension control.
- A robust control system.
- A fast and effective stamp mounting.

Although the system performed well in the above aspects, it lacks flexibility; in fact, the printing roller is fixed. This configuration guarantees high repeatability, but on the other hand, if misalignments of the printing module occur with respect to the other components of the system, it is not possible to adjust its position.

Moreover, in order to detect which are the components to improve or even to redesign, an error analysis was performed. The following error sources were identified to be those that most significantly affect the output printing quality:

- Non repeatability of the impression roller vertical motion.
- Inaccurate alignment of the stamp with the print roller.
- Not uniform stamp thickness.
- Lack of parallelism between the print roller and impression roller.

To improve the repeatability of the impression roller new high precision bearings were implemented. For detail of the design process refer to Wenzhuo Yang's thesis[29].

To improve the accuracy in alignment of the stamp on the print roller a new high precision wrapping system was designed and built. This system involves an innovative wrapping process using a magnetic sleeve and a magnetic stainless steel sheet used as support for the PDMS stamp. For detail of the design process refer to Charudatta Datar's Thesis[30].

To obtain a more uniform stamp thickness, a new stamp casting device was designed and fabricated. For detail of the design process refer to Yufei Zhu's Thesis[24].

Finally, the current machine does not offer the possibility to adjust the position of the print roller with respect to the substrate and the impression roller. This assures repeatability, but does not allow any adjustment in case of error. Therefore, to compensate any misalignments, a high precision positioning system for the print roller was designed. This system assumes a fundamental role in the multilayer printing process where the adjustability of the print roller becomes essential.

Details of the concepts generation, concept selection and the consequent design process are reported in chapter four of this thesis.

4.3   High Precision Positioning System: Synthesis Process

In the early stage of the project, in order to design the positioning system, a synthesis process articulated in the following phases was performed:

- o Recognizing a need.
- o Establishing design requirements.
- o Conceptualization and creativity.
- o Assessment of feasibility.

In particular, establishing quantitative requirements is an essential first step in the design   process. However, quantitative requirements were set before generating any concepts to leave the field open to any solutions.

4.4   Basic Specifications for the Design Process

To achieve higher quality in the single layer printing, the print roller and impression roller must be parallel and perfectly aligned. In fact, if there are any misalignments or not perfect parallelism, to ensure that impression and print roller are completely in contact along the printing line, the pressure distribution will not be uniform. This lack of parallelism causes deformations on the elastomeric stamp that result in distorted features transferred to the gold substrate.

In the multilayer printing process, these errors are still more critical. In fact, after having printed the first layer, the elastomeric stamp is changed and the substrate is rewound in order to print the second layer on the first one. Although the latter operations are carefully performed, errors will inevitably be introduced in terms of parallelism between the impression and print roller and between the print roller and substrate. To achieve high quality in the multiple layers printing process, it is necessary to compensate these errors in order to minimize misalignments between the first and second layer.
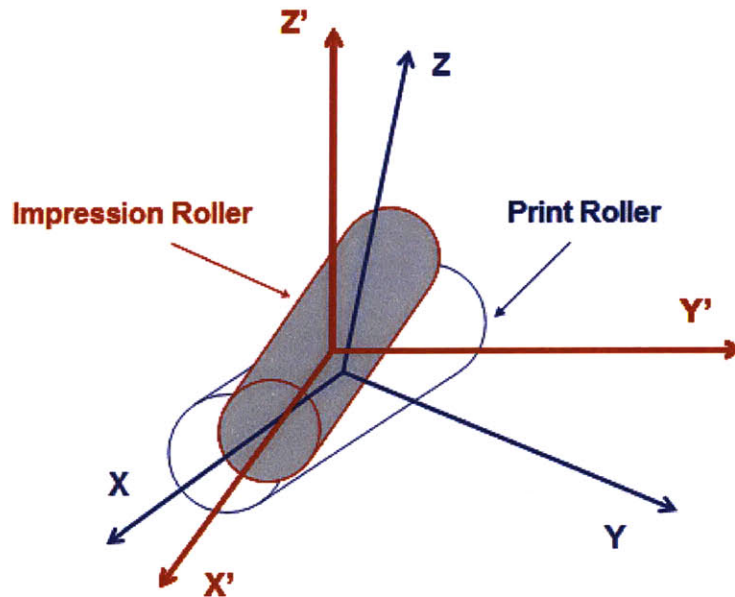
Figure 35: Possible Misalignments Between Impression Roller and Print Roller.

As can be seen from Figure 35, in the worst case, the impression roller and print roller might be misaligned along all six degrees of freedom.

However, for the single layer printing process, it is necessary to control only four degrees of freedom; in fact, impression roller is longer than the print roller and it does not have preferred orientation around x. Therefore, misalignment along the y is negligible and rotation around x has not effect. On the other hand, because in the multilayer printing process alignment between print roller and substrate is fundamental, then it is necessary to also control translation of the print roller along the y axis and rotation around x.

However, because rotation around x is controlled by the motor, then the positioning system needs to control the remaining five degrees of freedom listed below and shown in Figure 36:

1. Rotation about z.
2. Rotation about y.
3. Translation along x.
4. Translation along z.
5. Translation along y.
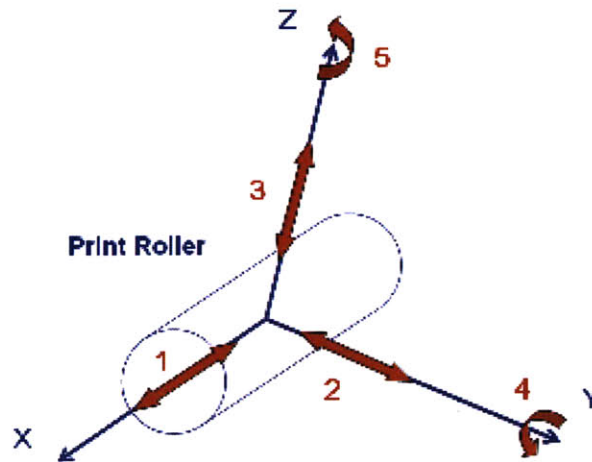
Figure 36: Degrees of Freedom Controlled by the Positioning System.

It was decided that the tolerable deformation in the monolayer printing must be contained within a five microns range. Moreover, misalignment errors in the multilayer printing must not exceed five microns. Therefore, to generate concepts, the following requirements were set:

1. The positioning system must not introduce new variability in the system.
2. The positioning system must control five degrees of freedom.
3. Resolution must be less or equal to five microns.
4. According to the resolution value, accuracy must be limited in order to remain in the five microns range.
5. Repeatability value must be limited in the five microns range.

4.5 Design Methodology

The design phase was critical in order to deliver a robust tool capable of controlling the position of the print roller with high repeatability and accuracy. It also needed to demonstrate the feasibility of manufacturing in a high production environment. During the design phase, to maximize utility and minimize time and cost, a strategy composed of the following points was followed:

- o Modularity:
  - Ability to adjust parameters quickly and easily.
  - Flexibility for testing and optimization.

- Design by part family:
    - Similar parts are faster and cheaper to produce.
    - Encourages modularity.

4.6 Concept Selection: Flexures

Final concept selection was made after several iterations; the selected idea involves the use of elastic supports, called flexures, which can be elastically deformed by applying forces on them. In fact, a flexure is an elastic mechanism consisting of a series of rigid bodies connected by compliant elements that is designed to produce a geometrically well-defined motion upon application of force[26]. Therefore, by applying forces on the flexures, which support both ends of the print roller shaft, these supports can be elastically deformed causing changes in the print roller position and orientation. A scheme of the proposed concept is illustrated in Figure 37.
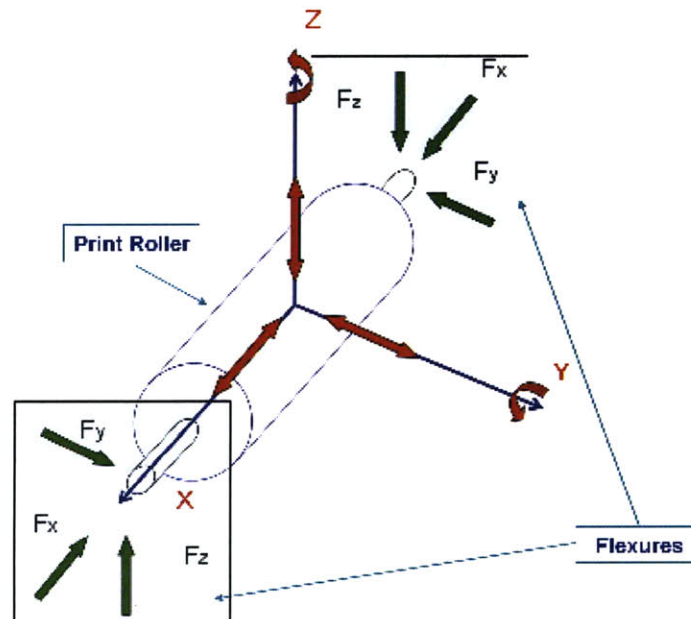
Figure 37: The Proposed Concept for the Positioning System.

4.7   Final Concept and Introduction to Flexure Design

In order to design the concept, two main problems have to be addressed:

1. How to apply forces on the flexures to provide controllable displacements.
2. How to decouple deformations along different axis.

Problem one is solved using micrometer heads, devices that are able to impose controllable displacements along one axis with high resolution, accuracy and repeatability.

Problem two is approached designing a particular flexure configuration which separates vertical and horizontal deformation and makes them independently controllable.

In this way, the print roller is located and oriented through rotations and translations generated by a combination of linear displacements imposed on the flexures using micrometer heads.

The final concept involves the use of two flexures as supporting system and five micrometer heads supported by other five fixtures. The CAD model of the final concept can be seen in Figure 38.
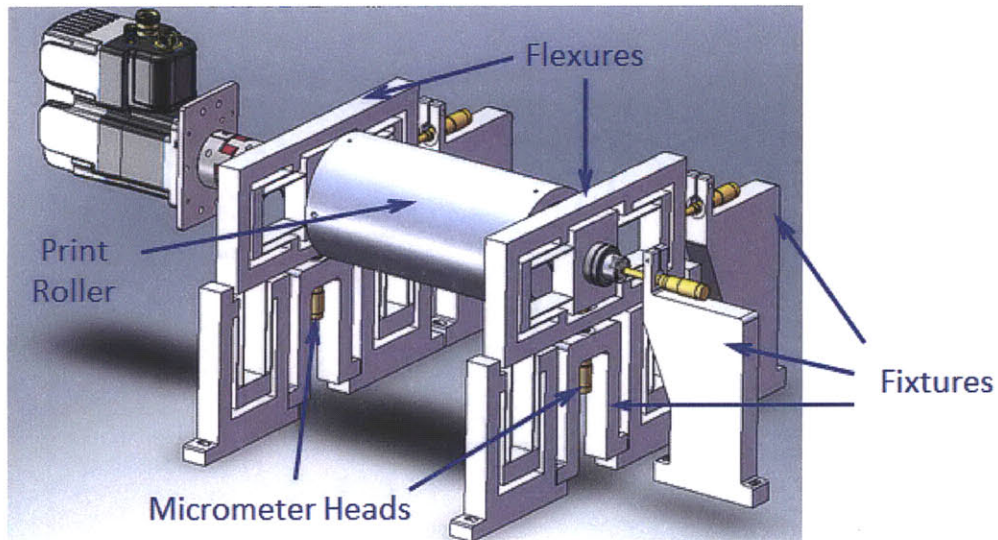
Figure 38: CAD model of the Proposed Final design of the Positioning System.

Before concluding this section, it is worthwhile to point out those considerations that make flexures the most suitable option as the core elements of the positioning system [25]:

- They are simple and inexpensive to manufacture and assemble.
- Unless fatigue crack develops, the flexure undergoes no irreversible deformations and are, therefore, wear-free.
- Complete mechanism can be produced from a single monolith.
- Failure mechanism such as fatigue and yield are well understood.
- They can be designed to be insensitive to thermal variations and mechanical disturbances (vibrations). Symmetric designs can be inherently compensated and balanced.
- There will be a linear relationship between applied force and displacement from small distortion. For elastic distortions, this linear relationship is independent of manufacturing tolerance. However, the direction of motion will be less defined as these tolerances are relaxed.

Nevertheless, the designer must not underestimate the following considerations during the design process:

- Accurate prediction of force-displacement characteristic requires accurate knowledge of the elastic modulus and geometry/dimensions. Even tight manufacturing tolerances can produce relatively large uncertainty between predicted and actual performance.
- At significant stresses, there will be some hysteresis in the stress-strain characteristic of most materials.
- Flexures are restricted in the length of translation for a given size and stiffness.
- Out of plane of stiffness tends to be relatively high in comparison to other bearing systems.
- They cannot tolerate large loads.
- Accidental overload can be catastrophic or, at least, significantly reduce fatigue life.
- At large loads there may be more than one state corresponding to equilibrium, possibly leading to instabilities such as buckling or "tincanning."

CHAPTER 5 – Positioning System Design

5.1 Introduction

The analysis of the function of the adjustment system and the design process and details of the new hardware are laid out in this chapter.

SOLIDworks 3D Computer Aided Design (CAD) software was used as the primary design tool. The ability to model individual components as well as assemble them in a virtual environment is powerful in designing complex machines. A great deal of other data can also be embedded in the files, such as engineering drawings and specifications, manufacturing tolerances, part numbering and revisions, vendor part numbers, Bills of Material (BOM's), etc.

5.2 Overview of the Positioning System Components and Functioning

The final design separates the different components into:

- o Back and front flexure: elastic mechanisms through which the system can be adjusted.
- o One central, two vertical, two horizontal micrometer heads : primary tools responsible for the fine adjustment.
- o Five fixtures to support the micrometer heads (two vertical, two horizontal and one frontal).

In Figure 39 a picture of the actual is shown. In the picture it is possible to recognize the different parts of the positioning system subassembly.
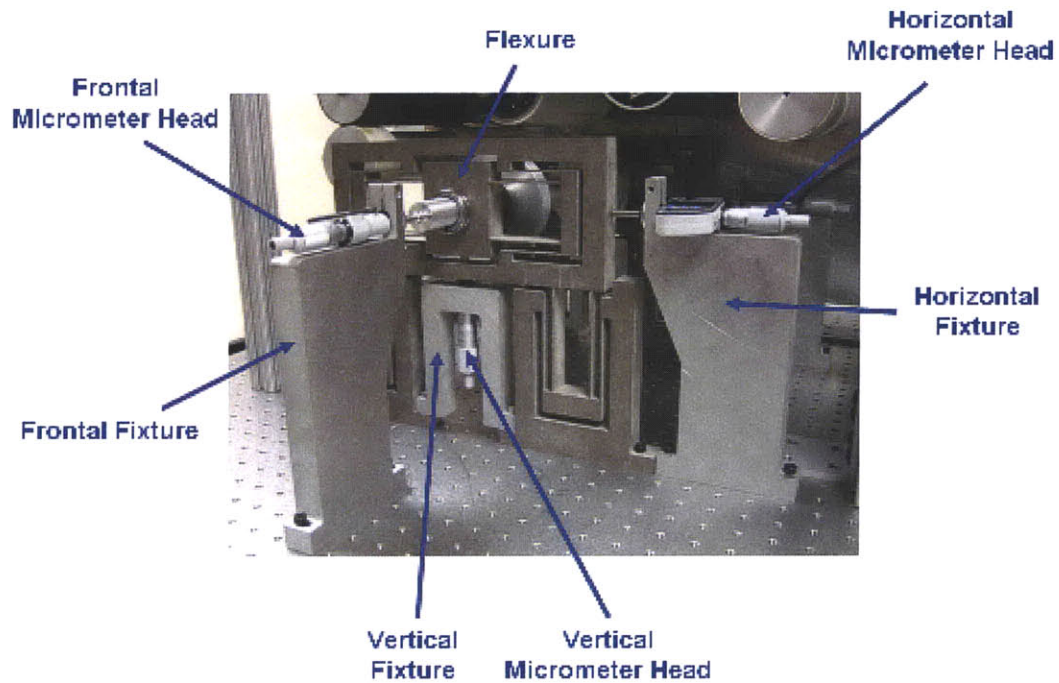
Figure 39: The assembled Adjustment System. The majority of custom components were manufactured by a local machinist and assembled by us at the NanoTerra facility.

Each component of the positioning systems is mounted on an optical table to ensure alignment with the other modules of the machine.

5.2.1 Print Roller Subassembly

The purpose of the positioning system is to control the position and the orientation of the print roller around five degrees of freedom. In order to thoroughly understand how the fine adjustment system works, the new print roller subassembly is briefly introduced:

The print roller subassembly is composed of the following parts:

a) Print roller shaft made of stainless steel 440C.
b) Thrust bearing.
c) Two linear rotary bearings.
d) Elastomeric Coupling.
e) Magnetic cylindrical sleeve on which the elastomeric stamp is wrapped.

The print roller is supported by two flexures; both ends of the print roller shaft are inserted in the flexures using two linear and rotary bearings (Figure 38c), which are press fit in the center hole of the flexures. These particular bearings allow the shaft to rotate and slide along the x axis. Finally the shaft is connected to the motor through a flexible elastomeric coupling (Figure 40d) which allows lateral, angular and axial displacements. A cross section of the print roller and the CAD model of its main parts are displayed in Figure 40a.
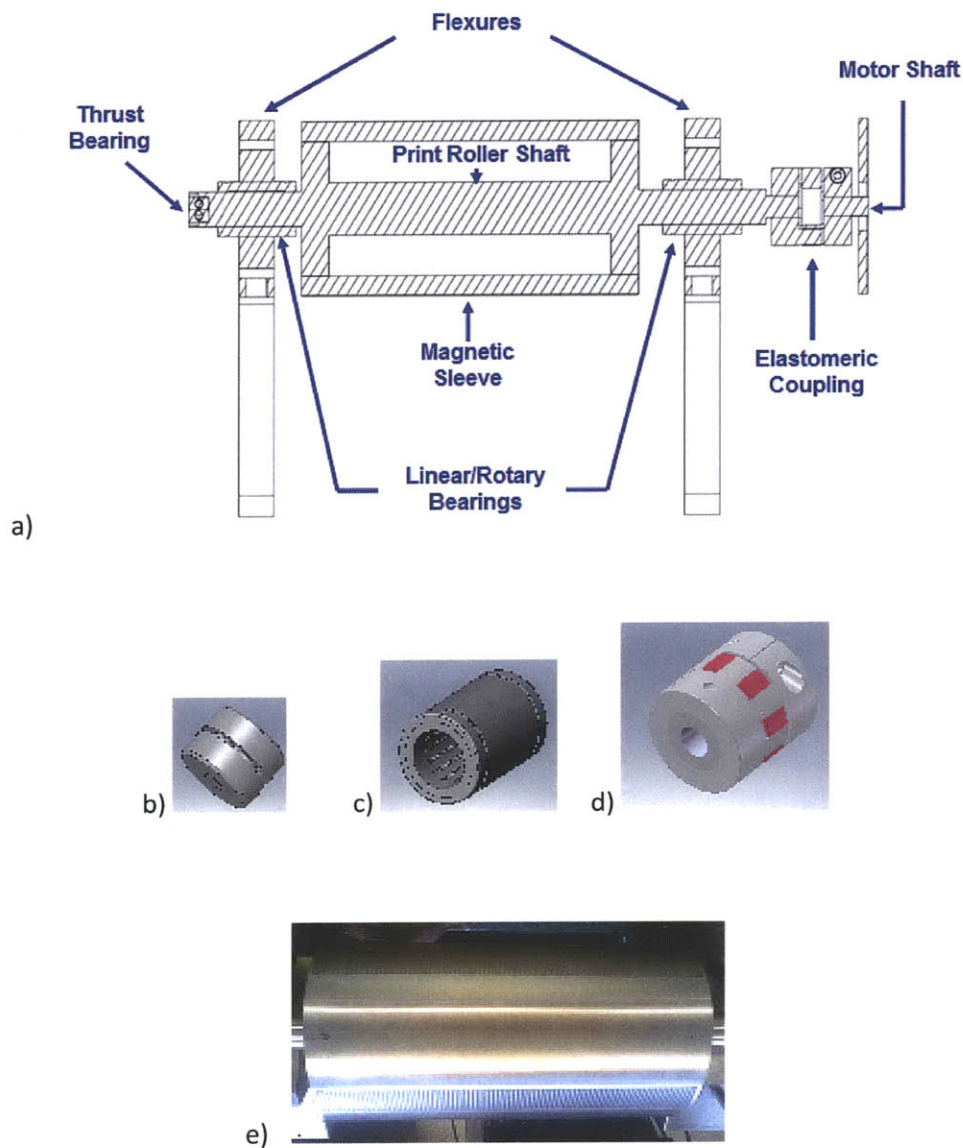
Figure 40: a) Cross Section of the Print Roller Subassembly Supported by the two Flexures; b) Thrust bearing, c) Linear/Rotary bearing, d) Elastomeric Coupling. e) Magnetic Sleeve mounted on the shaft.

The print roller consists of a magnetic sleeve attached to a shaft (Figure 40e) using setscrews. A magnetic backing plate with the PDMS stamp attached on it, is peeled and wrapped onto the magnetic sleeve using a new high-precision wrapping system. More details about this wrapping process can be found in Charudatta Datar's thesis [30].

The thrust bearing (Figure 40b) is press fit into the end of the shaft, which comes in contact with the micrometer head, enabling the x-axis registration system. This bearing decouples the rotation of the shaft from the micrometer head, preventing unwanted torques and stresses from developing.

5.2.2 Positioning System Functioning

The positioning system finely adjusts the position and the orientation of the print roller along five degrees through a combination of linear displacements. Fine linear displacements are imposed using micrometer heads; these devices are fixed with a clamp nut on fixtures and they are continuously in contact with the flexures; once the misalignment entities are determined, it is possible to accurately control their elongations by rotating the micrometer head stems. Consequently, micrometer heads elastically deform the flexures and set the print roller in a new position and orientations. In particular, vertical micrometer heads are responsible for translating the print roller along the z axis and rotating it around the y axis; at the same time, horizontal micrometer heads translates the shaft along the y axis and rotates the shaft around the z axis. Finally, the frontal micrometer head adjusts the print roller along x axis.

Once the position and orientation is determined, the micrometer heads are locked and they hold the flexures in the new configuration. At this point when the machine is turned on the print roller can rotate and the system flexures-micrometer heads behaves like a rigid system. Vibrations are damped by the coupling and by the flexures themselves.

The design and the detailed function of all the components composing the positioning system are discussed in the following section.

5.3   Flexure Design

Flexures represent the core part of the positioning system. These mechanisms can be elastically deformed along specific directions, while being stiff in other

directions[26]. Therefore, if properly designed, they can provide fine and smooth movements in definite directions.

In particular, flexures are designed giving them two degrees of freedom; in fact, they can be independently deformed along two linear and orthogonal directions. In this way, combining the action of the two flexures, it is possible to control the print roller along four degrees of freedom (rotation around y,z and translations along y,z); while, the fifth degree of freedom, adjustment along the x axis, is provided by the central micrometer head which loads the shaft along its own axis.

5.3.1 Flexure Design Process

According to the previous paragraph, the first step in the design process is to draw a particular configuration, which would make flexures independently deformable along two orthogonal dimensions; then, once the main structure is defined, the material is chosen and initial dimensions are set. At this point, through an iterative process based on a 3D finite element analysis, the final design is achieved.

Summarizing, the entire design process was performed according the algorithm schematized in Figure 41:
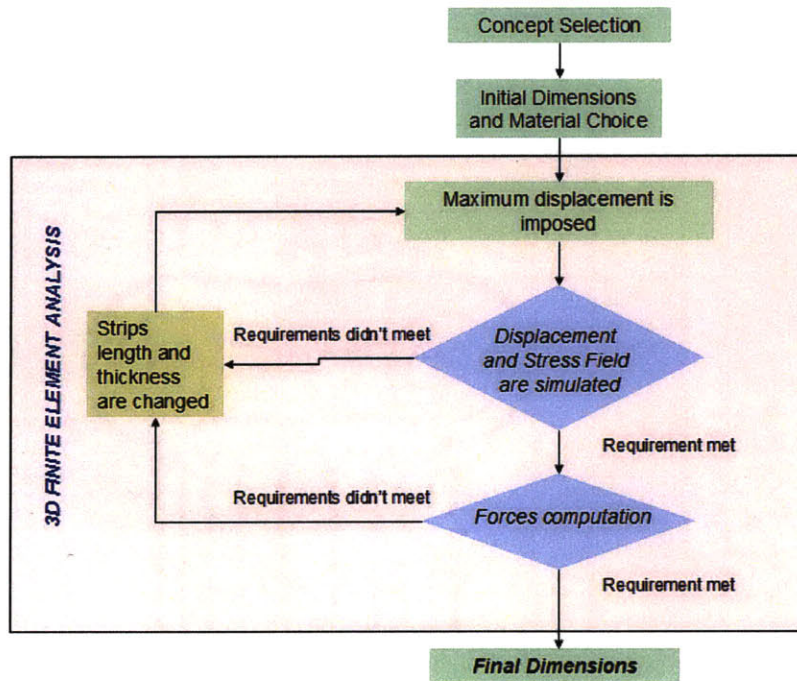
Figure 41: Algorithm Performed to Design the Flexures.

62

In the next paragraphs the reader will be guided through each step of the process shown in Figure 41.

5.3.2 Concept Selection

As stated earlier, the objective was to design an elastic mechanism that allows two decoupled motions along two orthogonal axes. In particular, the requirement was to design a specific configuration which when loaded along a definite direction provides a controlled displacement along the same direction. A sketch of the concept is shown in Figure 42.
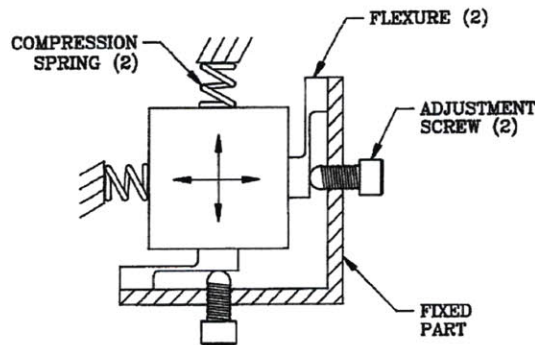
Figure 42: Proposed concept for the flexure representing a two-axis linear mechanism using flexures and screw actuators[16].

However, since the system relies on the flexure material elastic properties, it is not possible to displace the mechanism indefinitely. Therefore, to limit stress and to avoid unwanted or accidental displacements, which could permanently damage the flexures, mechanical stops are needed to restrict the range along which flexures can be deformed. In Figure 43, a typical mechanical stop configuration is illustrated.

Finally, the flexure configuration has to compensate for errors and disturbances and this can be achieved by designing a symmetric structure.
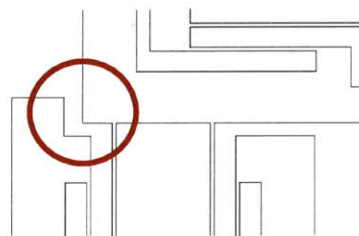
Figure 43: Typical Configuration of a Mechanical Stop Used in Flexures Design.

63

Summarizing, flexures structure must be designed meeting the following requirements:

- o Decoupled motions along two orthogonal axes.
- o Presence of mechanical stops to not overload the flexure.
- o Symmetry to compensate field disturbances.

Elaborating on the previous observations and requirements, the configuration displayed in Figure 44 was obtained as a result for both flexures:
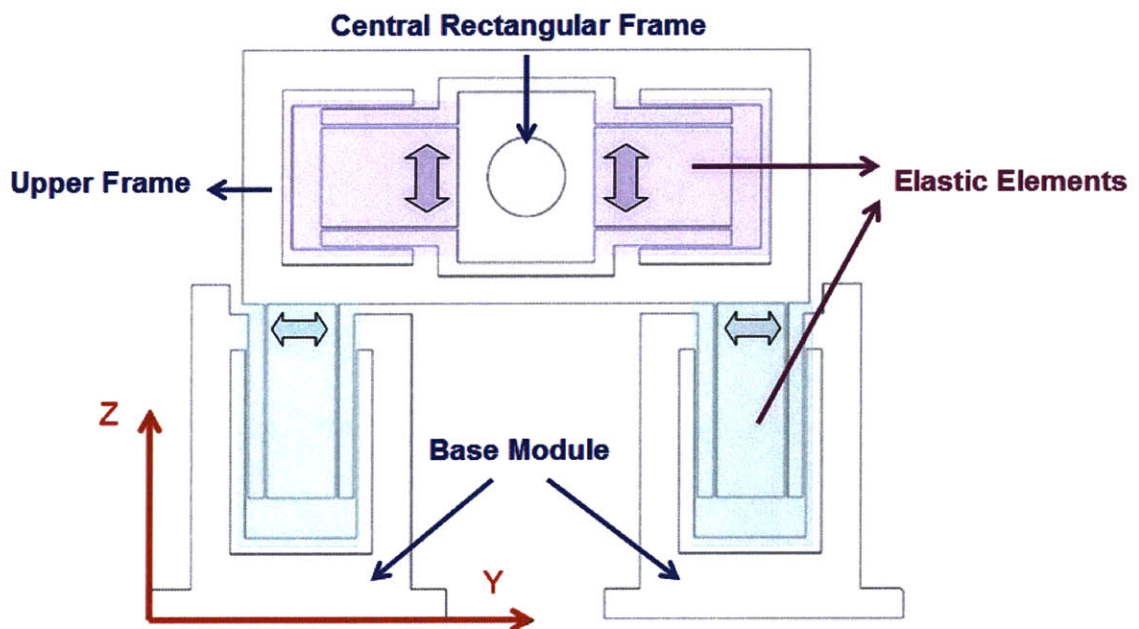
Figure 44: Final Design for the Flexures with its Main Subparts. In the figure the elastic elements have been highlighted. In particular, blue shadowed elements are responsible for the horizontal translation (along the y axis) of the Upper Frame, while violet shadowed elements provide the vertical translation (along the z axis) of the Central Rectangular Frame.

In particular, it must be pointed out that, obtaining an adequately high compliance ratio of the desired motion direction to that of the non-desired axis of deflection was achieved by dividing and separating the flexure into strips, thereby stiffening the system in the direction of separation without using more material [25].

In fact, as can be seen in the picture above, the flexure is mainly composed of three subparts: the base module composed of two elements screwed on the optical table, the upper frame, and the central rectangular frame. These three parts are

connected one with each other by four thin aluminum strips, which kinematically decouple the three parts.

Within the allowable range, if opportunely actuated the upper frame can translate along the y direction without influencing the base module, and at the same time the central rectangular frame can translate along the z axis without influencing the upper framework and the base module.

Finally, in the central rectangular there is a hole in which a linear / rotary bearing will be press-fit. This bearing will allow the shaft to translate along the direction perpendicular to the figure and to rotate at the same time when the machine is running.

5.3.3 Initial Dimensions and Material Choice

To guarantee repeatability and to avoid plastic deformation the flexure must work within 30% of its material elastic range. Therefore, in order to have wider flexibility, it is necessary to use a material with a broad elastic range. For these reasons and for its mechanical properties Aluminum 7075 T651 has been chosen. In fact, in the aluminum alloys family, this material is characterized by the higher yield strength (538 MPa).

As a first approach in dimensioning the system the following observations were followed [27]:

- o Motional errors are reduced by making the relative motion of individual flexure elements of the system small compared with their lengths.
- o Not bending the flexure over a radius less than 300 times its thickness.
- o The thickness of the flexures is restricted to one inch, due to the manufacturing process limitations.

5.3.4 3D Finite Element Analysis

The final dimensions of the flexure were achieved through a three dimensional finite elements analysis iterative process articulated as follows:

- The maximum displacement is imposed.
- The correspondent displacement and stress fields are calculated.
- If the max stress and the displacement field meet the requirements the design is finalized, otherwise the system will be modified until requirements will be meet.

In particular, the displacement field must meet the following requirements:

- Flexures must allow at least +/-2000 microns range of adjustment.
- Flexures configuration must allow the above range of elongation.

The stress field must meet the following requirements:

- Under the system of forces applied to the flexure the maximum stress must not exceed the 30% of the Aluminum 7075 T651 elastic field.
- The material must accomplish the desirable elongation under loads less than 150 N.

At this point if the maximum stress does not exceed the 30% of the aluminum 7075 yield strength and the overall displacement is feasible with the flexure configuration the design is considered final. Otherwise, the thickness and the length of the strips are changed and the process is repeated.

The strips length l and the coefficient of elasticity E are those parameters that can be adjusted to arrive at a given flexure specification [28].

Longitudinal deformation Δl of a single uniform member placed in tension or compression is calculated using the following equation:

$$\Delta l = F \cdot \frac{l}{A \cdot E}$$

where F is the change in applied force, l is the length of deformable interval, A is the cross sectional area of flexure and E is Young's modulus of elasticity from the material.

As can be seen from Figure 45 on each flexure are mainly applied two forces:

- The vertical micrometer applies is load direct under the central rectangular frame along the z axis.
- The horizontal micrometer applies is load to the upper frame along the y axis.
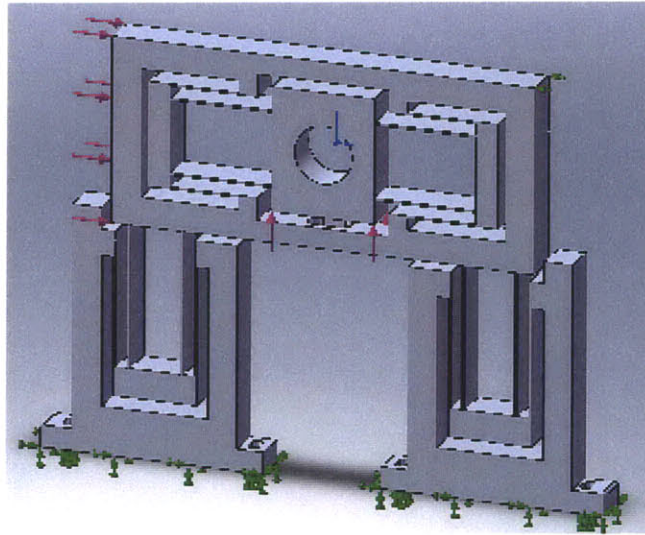
Figure 45: Scheme for Rigid Body Dynamics for the Flexure.

The iterative process is performed with the help of COSMOSWork, a SOLIDWork application that enables faster, less costly, and more optimized product development, as well as more in-depth examination of product performance than would ever be possible using even the most detailed prototypes.

The displacement and stress fields of the final design of the flexure are reported in Figure 46 and Figure 47:
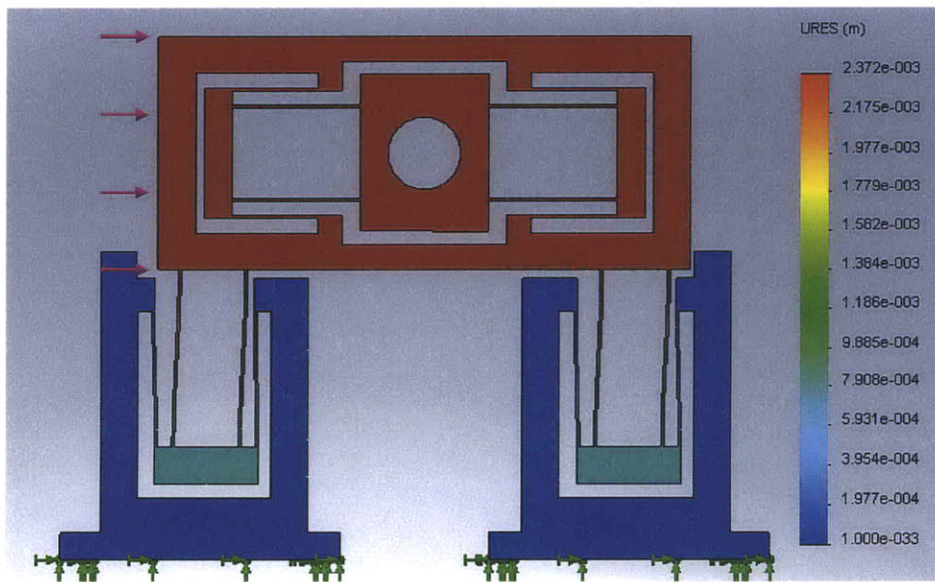
Figure 46: Displacement Field along y Axis for the Flexure when the Maximum Load is applied.
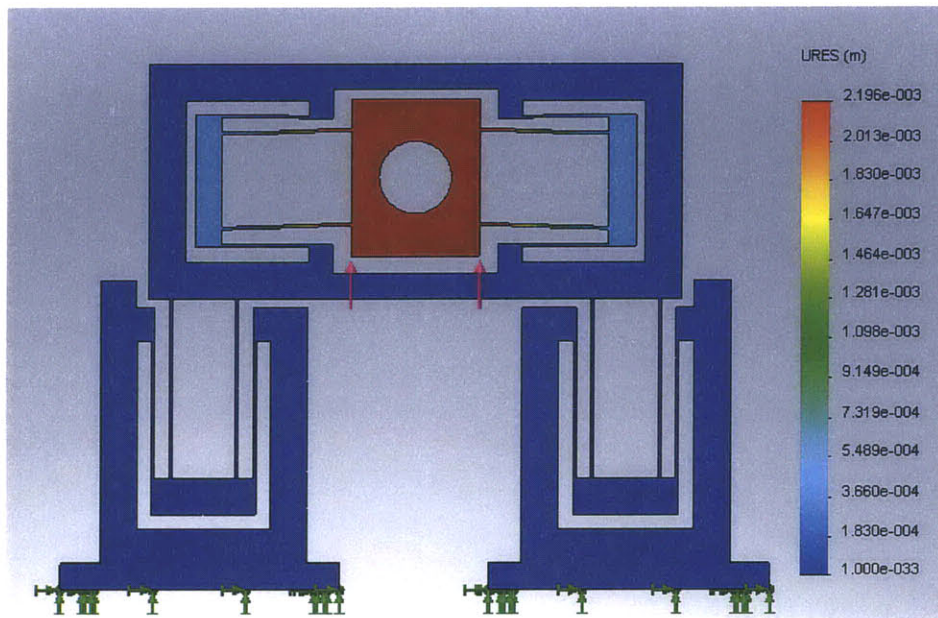
Figure 47: Displacement Field along z axis for the Flexure when the Maximum Load is applied.

Under the application of a load along y, the upper frame and the base part are completely decoupled. The base module is colored in blue and according to the legend in the figure, its displacement is negligible, while the upper frame is moving as a rigid body. This is achieved thanks to the thin aluminum bars which separate the two main modules.

Moreover, applying a force to move the central rectangular frame does not provide motion to the other part of the flexure: the upper frame and the basement module are blue: their displacements are negligible.

Finally, as it is shown by Figure 48, when the maximum displacement is applied along the y and the z axis, the maximum strength (98.34 MPa), is recorded along the thin aluminum bars which connect the central rectangular with the upper frame. However, the max stress registered during the simulation is significantly less than 30% of the elastic field (Aluminum 7075 T651 yield strength is 538 MPa).
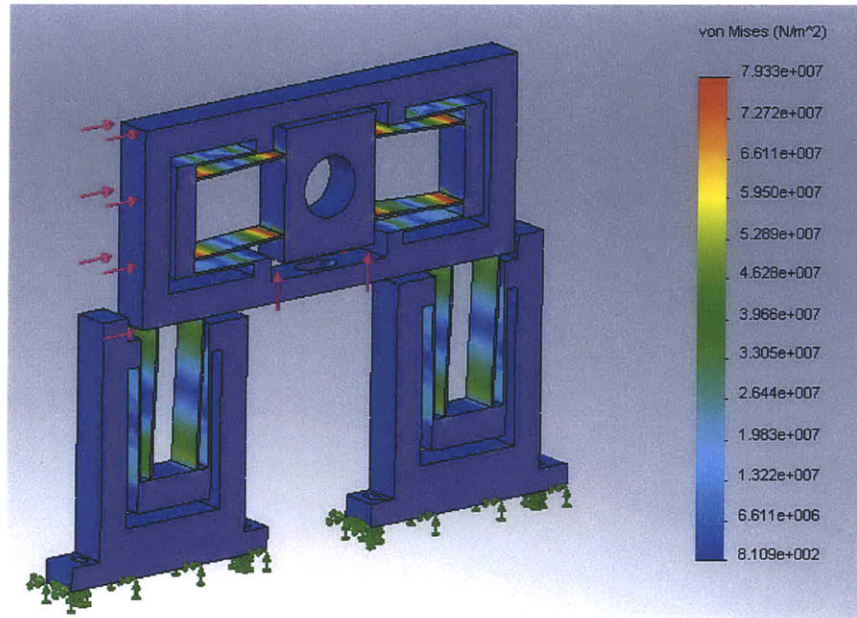
Figure 48: Overall Stress Field when Maximum Loads are applied on the Flexure.

Table 2: Load Applied by the Micrometer Heads, Maximum Displacements and Stresses Obtained in the Final Design of the Flexure.

Axis	Max Displacement	Max Stress	Force to apply
Y	2372 microns	50.09 MPa	50 N
Z	2196 microns	98.34 MPa	120 N

5.4 Micrometer Heads

By definition, a flexure mechanism produces defined displacements upon application of forces. In this case, forces are applied by micrometer heads continuously in contact with the flexures; in fact, micrometer heads, are devices used widely in mechanical engineering and machining to impose repeatable, accurate and controllable displacements.

In the micrometer heads selection of the following requirements were fixed:

- o Resolution coupled with accuracy must be less than 5µm.
- o Vertical micrometers will support the entire load of the print roller, therefore they must work under heavy duty.

Following the observations above the following micrometer heads have been selected:

- o Vertical micrometer head: Mitutoyo 151-237, resolution 2.5µm and accuracy 2.5µm (Figure 49).
- o Horizontal and frontal micrometer head: Mitutoyo 350-352, resolution 1µm and accuracy 2.5µm (Figure 50).

Figure 49: Mitutoyo 151-237. Mitutoyo America Corporation[31].

Figure 50: Mitutoyo 350-352. Mitutoyo America Corporation[31].

5.5 Fixtures

Fixtures have an essential function in the positioning system since they support and orient the micrometer heads. Fixtures need to be accurately designed, in fact in case of non- orthogonality, unwanted torques might be generated on the flexures. In general, the following objectives are taken into account while designing fixtures:

- o Under the applied load stress must not exceed the elastic limit.
- o Under the applied load the maximum displacement along the load direction must not exceed five microns.
- o Easy eyes and hands accessibility.

5.5.1 Design Process

The design process is articulated as the algorithm shown in Figure 51 :
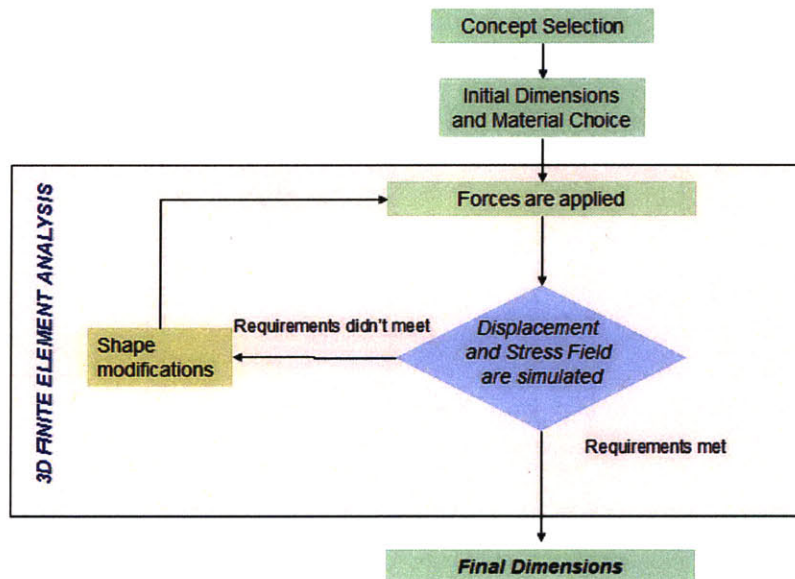
Figure 51: Algorithm Performed to Design the Flexures.

5.5.2 Concept Selection

According to their different application three kinds of fixtures were designed:

- o Vertical fixture (Figure52).
- o Horizontal fixture (Figure53).
- o Frontal Fixture (Figure54).

Vertical fixture support micrometer heads that introduce displacement along z. These micrometer heads support the load of the print roller. Therefore, since there are two vertical micrometer heads, the vertical fixture a load on each is one- half of the print roller weight plus the force necessary to displace the flexure.

Figure 52: One of the Two Vertical Fixtures Assembled in the Frontal Flexure.

Horizontal fixtures support the micrometer head, which introduces displacement along y. On the horizontal fixture only the force necessary to displace the flexure along the y axis is applied .
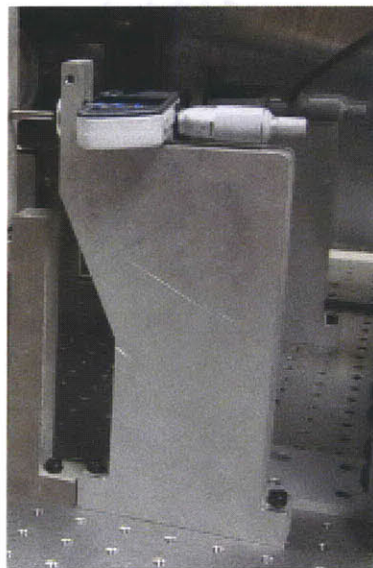
Figure 53: One of the Two Horizontal Fixtures Screwed on the Optical Table.

72

Finally, the central fixture is structurally equal to the horizontal one, but he is used to control the position of the print roller along the x axis (transverse to the roller). Since the load applied on the central fixture is of the same order of the load applied to the horizontal fixtures, in the following paragraphs the attention will be focused only on the vertical and horizontal design processes.

Figure 54: Central Fixture; the Micrometer Head Supported by this Fixture Adjusts the Position of the Print Roller along X.

5.5.3 Initial Dimensions and Material Choice

The initial dimensioning of the fixtures are performed taking into account their positions with respect to the flexure and the fact that they must allow eyes and hands accessibility to set the micrometer heads.

Aluminum 6061 T651 is selected as the ideal material for the force applied. The yield strength of this material is 241 MPA.

5.5.4 3D Finite Element Analysis

The final design of the fixtures must meet the following requirements:

- o Under the application of the maximum load no plastic deformation must take place. Max stress must not exceed the 30% of the elastic range.
- o Displacements due to the applied load must not exceed three microns.

The final dimensions of the flexure were achieved through a three dimensional finite elements analysis iterative process articulated as follows:

- o According to the results obtained in the flexure design the loads are applied on the fixtures.
- o The stress and displacement field are computed.
- o If the max stress and the displacement field satisfy the requirements the design is finalized, otherwise the system will be modified until the requirements are met.

5.5.5 Vertical Fixture Design

Vertical fixtures hold the micrometer head that will push the print roller along the z axis. As computed in the flexure design section, the necessary force to obtain the wanted displacement is 120 N. However, this micrometer head also supports the print roller weight (150 N). The two vertical micrometer heads will equally share the total weight of the print roller. Therefore, each vertical micrometer head will apply on the fixture a load of 75 N to support the print roller plus a load of 120 N when the maximum displacement is requested.

Consequently, to design the vertical fixture, it has been loaded with a 195 N load. A scheme of rigid body dynamics is shown in Figure 55.
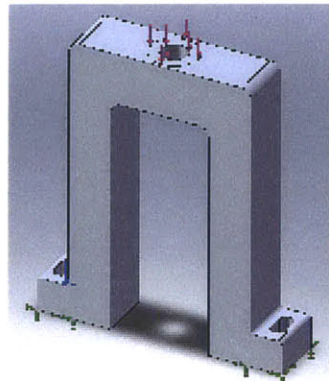
Figure 55: Scheme of Rigid Body Dynamics of the Vertical Fixture.

Stress and displacement diagrams (Figure 56 and Figure 57) show that that the maximum strength and displacement is achieved around the hole for the micrometer head:

a)

b)
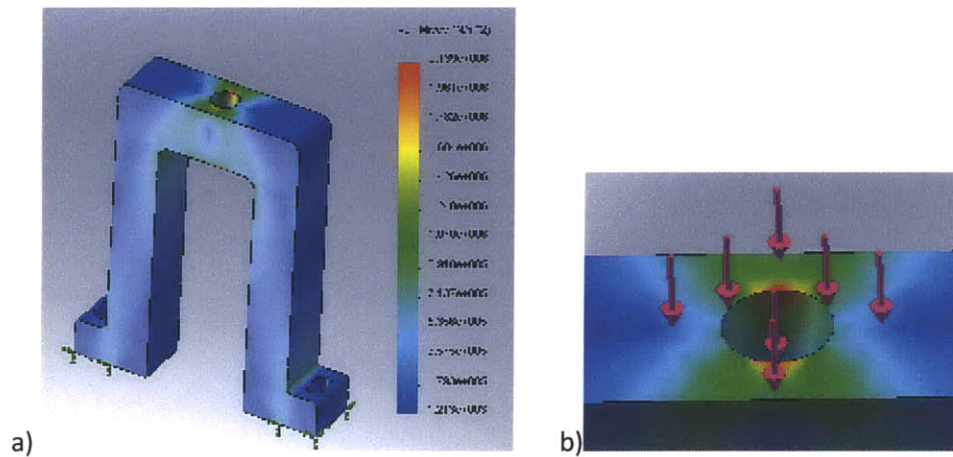
Figure 56: a) Stress Field in the Vertical Fixture; b) Maximum Stress is Registered Around the Hole where the Micrometer Head will be Slid Fit.
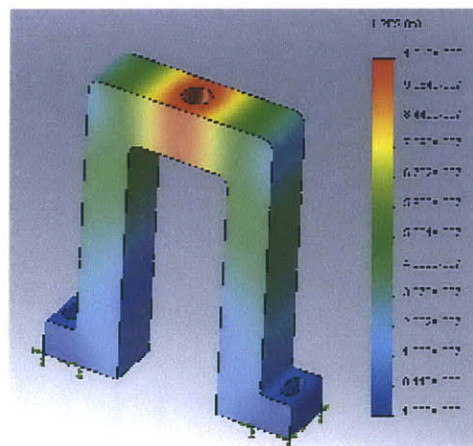
Figure 57: Displacement Field for the Vertical Fixture.

Table 3: Load applied on the vertical fixture, maximum displacement and stress obtained in the final design of the vertical fixture.

Axis	Force applied	Max Displacement	Max Stress
Z	195 N	1.013µm	2.14 MPa

The maximum strength achieved (2.14MPa) is less than the 10% of the yield strength so plastic deformation is totally avoided.

5.5.6 Horizontal Fixture Final Design

A similar approach was followed for the horizontal fixture and the frontal fixture. Their diagrams follow (Figure 58):
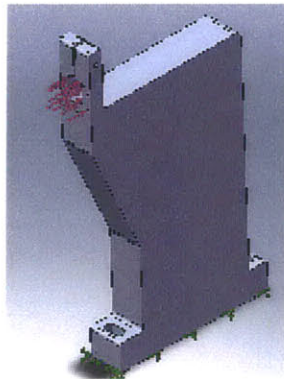
Figure 58: Scheme of Rigid Body Dynamics of the Horizontal Fixture and Frontal Fixture.

In the flexure design section it has been shown that to impose the maximum displacement along the y axis, flexure must be loaded with a 50 N load.
Studying the stress and displacement fields shown in Figure 59 and Figure 60, it has been observed that, under the application of a 50 N load, the maximum stress registered is 1.41 MPa and the maximum displacement recorded is 4.34µm. Both values successfully meet the specifications.

a) b)
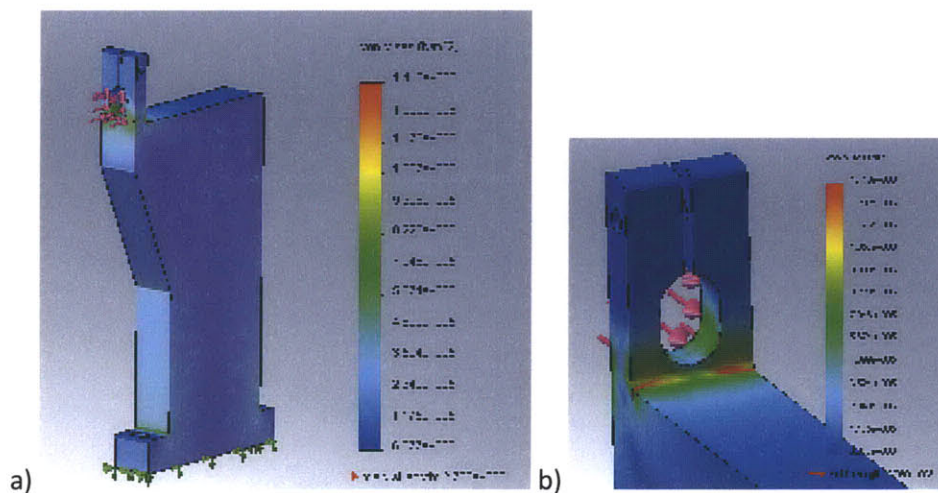
Figure 59: a) Stress Field in the Horizontal Fixture; b) Maximum stress is Registered at the Corner Between the Fixture Body the Clamp.
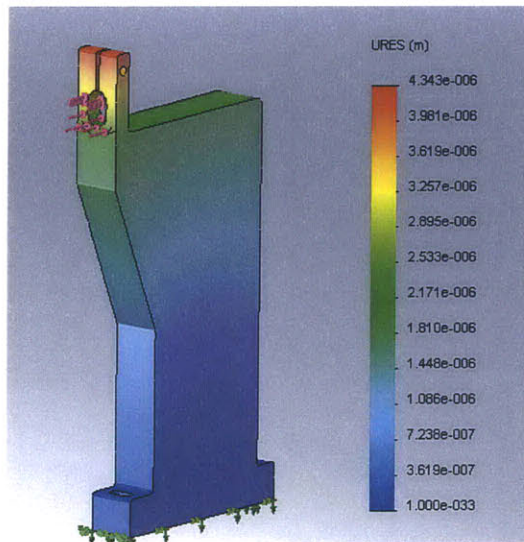
Figure 60:Displacement Field for the Horizontal Fixture.

Table 4: Load Applied on the Horizontal and Central Fixture, Maximum Displacement and Stress Obtained in the Final design of the Horizontal Fixture.

Axis	Force applied	Max Displacement	Max Stress
X	50 N	4.34 microns	1.41 MPa

5.6 Installation and preload of the Positioning System

Each flexure has two degrees of freedom. In particular, using micrometers it is possible to provide independent displacements along the y and z axis. However, given the structure of the system, the micrometer can push only towards one direction. Therefore, to guarantee a symmetric range of adjustment it is necessary to preload the flexure. For example, in this case the total desired range of adjustment is +/- 1000 microns and to use the full range it is necessary to preload the flexures with a displacement of 1000 microns and set this position as the "zero displacement" position called "home position" (Figure 61). In this way, micrometer heads can be used in both positive and negative directions; at this point, is it still possible to compress the flexure having a positive displacement or decompress the flexure retracting the micrometer head having a negative displacement. In fact, retracting the micrometer will cause the flexure, due to the elastic properties of the material, moving back to its zero stress position.

This operation is essential to correctly dimension the flexures. In fact they must be designed in order to allow displacement at least two times wider than the desired adjustability range. For example, in this case the flexure was designed for a maximum displacement of 2000 microns.
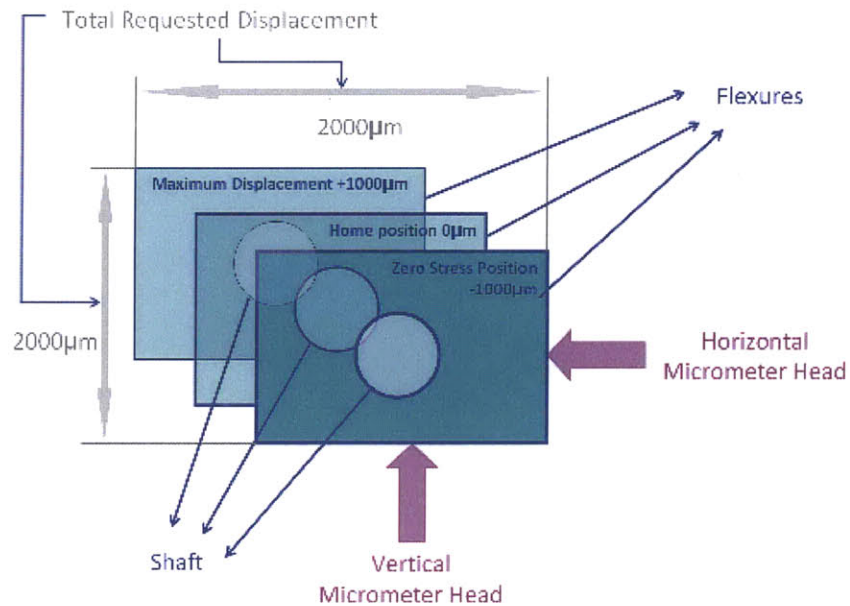
Figure 61: Flexure Installation.

Aluminum is a soft material, while the stem of the micrometer is made of stainless steel. To ensure repeatability of the positioning system, it is necessary to avoid any scratches or surface deformation of the flexures surface by the micrometer heads. Therefore, a small stainless steel surface was attached to the flexure where the micrometer head applies its load. Moreover, to avoid the non parallelism of the micrometer head face with the flexure, the micrometer heads were augmented with a hemispherical head (Figure 62).

Figure 62: Stainless Steel Surface Attached to the Flexure to Avoid Permanent Deformation.

CHAPTER 6 – Calibration and Performance

6.1 Introduction

Once mounted on the optical table, the positioning system was tested and calibrated. As explained in detail in the first chapter, the designed system is able to control five degrees of freedom. Ideally, each adjustment along one axis should be decoupled from the other axes. However, in real systems coupling among controlled axes is generally expected. Therefore, to identify the coupling entity among all five axes calibration was performed.

6.2 Calibration of the System

The calibration is executed with the entire system as a black box and focusing only on inputs and outputs as represented in Figure 63.
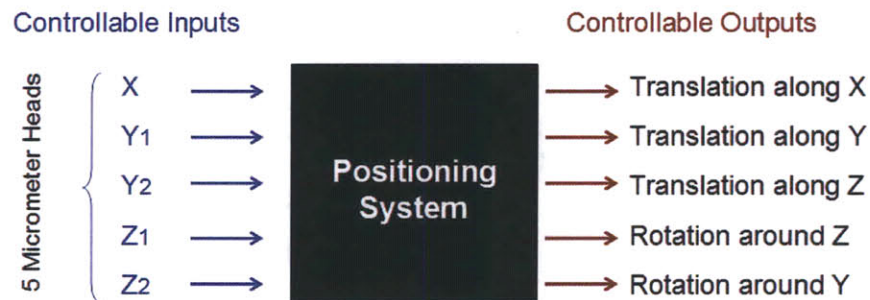
Figure 63: Positioning system as a black box during the calibration phase. Rotation around the x axis is not considered as an output. In fact, the print roller rotation is controlled by the motor.

As can be seen from the Figure 63, the positioning system is characterized by five inputs and five outputs. In particular, inputs are represented by micrometer heads while outputs are the position and the orientation of the print roller. Displacements of the print roller were recorded using digital dial indicators (Figure 64).
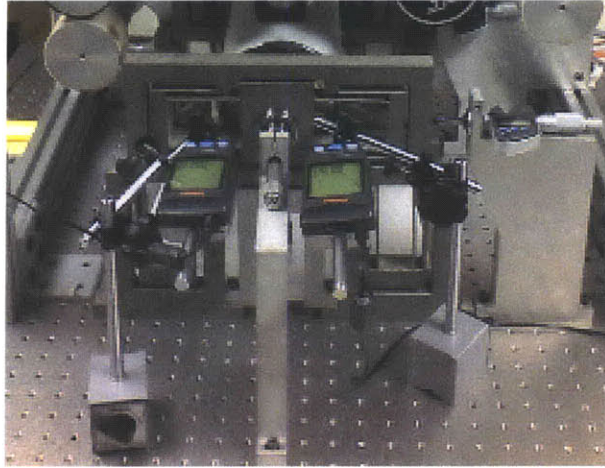
Figure 64: In this picture a couple of linear indicators are recording the output along the x axis.

6.3   Calibration Matrix

The goal of the calibration phase is to find the relationship between inputs and outputs. This relationship can be expressed by a matrix equation as follows:

$$[Output] = [A] \times [Input]$$

Figure 65: Compact matrix equation inputs-outputs

where [Output] and [Input] are vectors with dimension equal to five. While, A matrix, with a 5x5 dimension, represents the relation inputs-outputs. Symbolically, matrix A represents the functioning of the black box drawn in Figure 63. The extended matrix equation is reported in Figure 66.

$$\begin{bmatrix} O_1 \\ \cdot \\ \cdot \\ \cdot \\ O_5 \end{bmatrix} = \begin{bmatrix} a_{11} & \cdot & \cdot & \cdot & a_{15} \\ \cdot & \cdot & \cdot & \cdot & \cdot \\ \cdot & \cdot & \cdot & \cdot & \cdot \\ \cdot & \cdot & \cdot & \cdot & \cdot \\ a_{51} & \cdot & \cdot & \cdot & a_{55} \end{bmatrix} \times \begin{bmatrix} I_1 \\ \cdot \\ \cdot \\ \cdot \\ I_5 \end{bmatrix}$$

Figure 66: Extended Matrix Equation Inputs-Outputs

In ideal cases when each axis is decoupled from the others, matrix A assumes a diagonal form as shown below in table 5; while in real cases off-diagonal terms are not zero and their magnitudes supply an information about coupling among axes.

Operatively, matrix A might be seen as an efficiency indicator of the positioning system. In other words, the more the off-diagonal terms are closer to zero the more the positioning system is efficient and controllable.

Table 5: Typical Calibration Matrix for Ideal Systems.

	X	Y	Z	rot Y	rot Z
X	1	0	0	0	0
Y1	0	1	0	0	0
Y2	0	0	1	0	0
rot Y	0	0	0	1	0
rot Z	0	0	0	0	1

In the current system, as explained in detail in the previous chapter and as shown in Figure 67 the five degrees of freedom are controlled through combinations of linear displacements and there are no inputs that impose pure rotations; therefore, the ideal calibration matrix for the current system will be slightly different. In addition, since input Y_1- Y_2-Z_1- Z_2 are not applied to the center of mass of the print roller, as can be seen in Figure 67 and Figure 68 rotational couplings will be present.
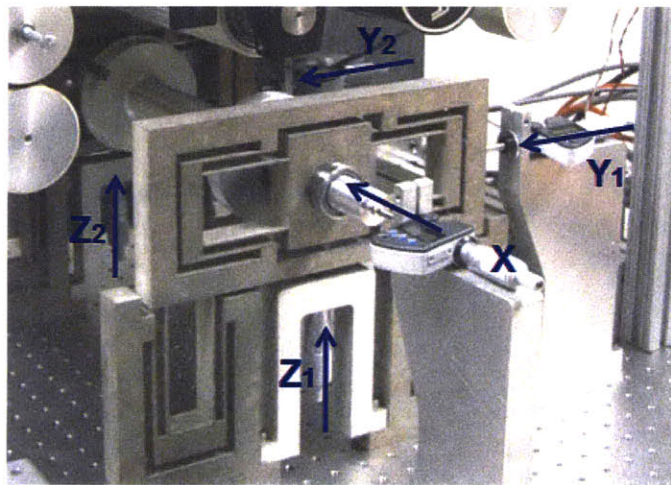
Figure 67: The Five Inputs of the Adjustment System.
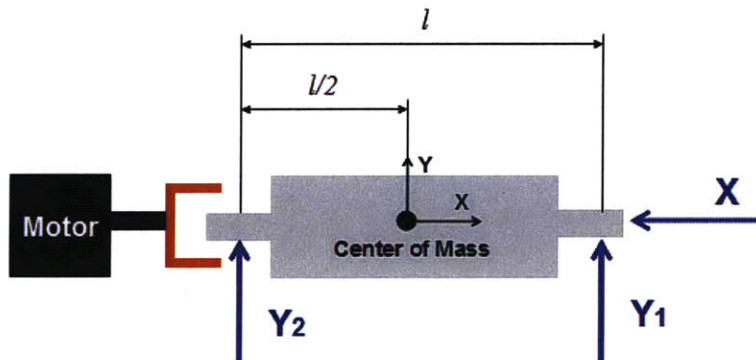
Figure 68: Scheme of the System. Micrometer heads are not applied to the center of mass of the roll. Therefore, rotational couplings will be present and their values will be as shown in Table 6.

In this case, if the system was ideal it would be characterized by a diagonal calibration matrix as shown in Table 5:

Table 6: Ideal Calibration Matrix for the Current Positioning System.

	X	Y	Z	rot Y	rot Z
X	1	0	0	0	0
Y1	0	1	0	0	$\arctan(y_1/(l/2))$
Y2	0	1	0	0	$\arctan(y_1/(l/2))$
Z1	0	0	1	$\arctan(z_1/(l/2))$	0
Z2	0	0	1	$\arctan(z_2/(l/2))$	0

6.4 Assumptions

Calibration is performed based on the following assumptions:

a) As long as the displacement imposed by micrometer heads is within the elastic range, flexure has a linear response.
b) The effect of the two flexures is symmetric with respect to the center of the print roller.
c) The print roller is a completely rigid body.
d) Flexure parasitic errors are negligible.

According to assumption b, experiments were run only considering inputs X-Y_1-Z_1 and assuming that inputs Y_4 and Z_2 generate the same effect as Y_1 and Z_1.

According to assumption c, during the calibration process, it is necessary to monitor and record only the position and the orientation of one point. Operationally, the displacements were recorded in accessible points of the system, then data were referred to the center of the print roller (Figure 69).
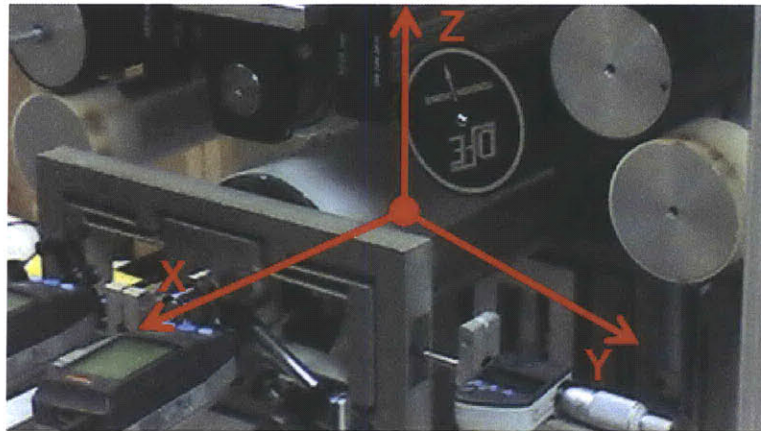
Figure 69: Reference System Used During the Calibration.

6.5 Experiments

To determine matrix A, experiments were designed and performed according to the following steps:

1) The print roller is set in its "home position" and " home orientation". As previously explained the home position of the print roller is that position in which both ends of the shaft are preloaded in the center of the designed flexure range.
2) One input is introduced setting all the others equal to zero.
3) Through dial indicators the effect of the introduced input is analyzed in terms of displacement along the controlled five degrees of freedom.
4) To clear the data from uncontrollable fluctuations three runs are performed for each experiment.
5) Steps 1 through step 5 are repeated for all five inputs.

6.6 Calibration Results

The results obtained are listed below in Table 6:

Table 7: Results Recorded by the Dial Indicators. It is important to note that, displacements of the system were recorded using digital linear dial indicators. Therefore, in order to measure rotations were used couples of indicators on each axis and they were called: Y_1, Y_2, Z_1, Z_2, X_1, and X_2.

				Displacements measured by Dial Indicators (mm)					
				Y1	Y2	Z1	Z2	X1	X2
INPUTS (mm)	I₁	X	-1.0000	0.0000	0.0000	0.0000	0.0181	-0.8433	-0.8417
	I₂	Y1	-1.0000	-0.8849	-0.1468	0.0000	0.0411	0.1480	-0.1422
	I₃	Z1	1.2700	-0.0004	-0.0419	0.4150	0.0476	-0.0713	-0.0008
	I₄	Y2	-1.0000	-0.1468	-0.8849	0.0411	0.0000	-0.1422	0.1480
	I₅	Z2	1.2700	-0.0419	-0.0004	0.0476	0.4150	-0.0008	-0.0713

Using the data above, matrix A was constructed (Table 7). In particular, to obtain a normalized matrix, data were normalized over the displacement that caused them.

Table 8: Calibration Matrix A for the Actual System.

		OUTPUTS: 5 Degrees of Freedom				
		O₁	O₂	O₃	O₄	O₅
		X	Y	Z	rot Y	rot Z
5 CONTROLLABLE INPUTS	X	0.84	0.00	-0.01	-1.57	0.00
	Y₁	0.00	0.88	-0.02	-1.57	1.57
	Y₂	0.00	0.88	0.08	1.57	-1.57
	Z₁	-0.03	-0.02	0.33	-1.57	1.57
	Z₂	-0.03	-0.02	0.33	1.57	-1.57

Results show that the matrix has not the ideal configuration. In particular, non-expected linear and rotational couplings have been displayed in yellow. Moreover, expected rotational couplings assume larger magnitudes than forecasted because the print roller is connected to the motor through an elastomeric coupling with limited lateral displacement. Therefore, when the imposed displacement exceeds the maximum elastomeric coupling lateral displacement, a larger rotation is generated as shown in Figure 70. Obviously, the latter does not happen when the print roller is loaded along its own axis, the x axis, by the central micrometer head; in fact, in this case, the elastomeric coupling is not laterally loaded.
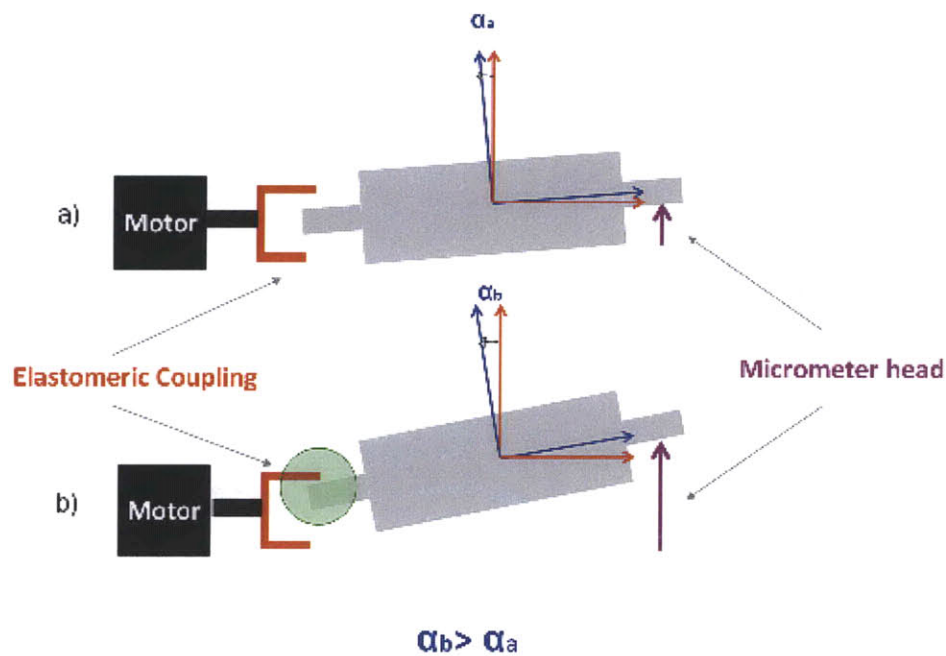
Figure 70: a) Displacement imposed does not exceed the maximum lateral coupling misalignment; b) The displacement introduced as input, by the micrometer head, exceeds the allowable coupling lateral misalignment; in this case the rotational coupling assume a larger value.

As shown in Table 6, calibration was performed introducing inputs that exceed the allowable later coupling misalignment. Therefore, rotational couplings assume significant magnitudes. However, it is worthwhile to point out that the magnitude of each rotation is exactly the same, which shows the repeatability and the accuracy of the positioning system.

Finally, it has been obtained that in the worst case the system shows a coupling between y and z axis only of 8%. Considering the fact that the calibration was

performed introducing as input the full range for which flexures were built, the performance of the flexure can be considered adequate.

In conclusion, it is necessary to point out that, in general it is not common to introduce such as wide displacements as inputs; on the contrary, micrometer heads will be only used to finely adjust the print roller within a range of 50-100 microns. This range lies within the allowable coupling lateral misalignment, therefore, in normal cases rotational couplings will not be as large as they were recorded during the calibration. Moreover, in case of smaller displacements, it will not be surprising if also linear coupling would be shorter. In fact, on the current system the calibration was performed imposing the full range ($\pm 1000\mu m$) and this occurrence, since the flexures are entirely constrained only along the directions where the micrometer heads are applied, makes the one side accumulation of errors, more likely to take place.

6.7 The Importance of Calibration Matrix in the Multilayer Printing Process

When matrix A is known the positioning system is completely defined and controllable. In fact, knowing A, is possible to place the print roller exactly at any desired positions. Indeed, simply inverting matrix A is possible to compute the input vector which is necessary to insert to place the roller in a given position and orientation.

$$
\begin{bmatrix} I_1 \\ . \\ . \\ . \\ I_5 \end{bmatrix} = \begin{bmatrix} a_{11} & . & . & . & a_{15} \\ . & . & . & . & . \\ . & . & . & . & . \\ . & . & . & . & . \\ a_{51} & . & . & . & a_{55} \end{bmatrix}^{-1} \times \begin{bmatrix} O_1 \\ . \\ . \\ . \\ O_5 \end{bmatrix}
$$

Figure 71: Matrix Equation Inputs-Outputs. Essential to quantify the input to introduce to place the system in the desired position and orientation.

The matrix equation shown in Figure 71 takes an essential role in the multilayer printing process. Multiple layers printing process consists of printing several times the first layer along the length of the gold substrate, rolling back the gold web, and printing again the second layer.

High quality in this process is achieved minimizing misalignments between features of the first and the second layer. At this purpose, the above matrix

equation allows the operator to compensate those misalignments finely adjusting the position of the print roller with respect to the first layer.

In fact, after having printed the second layer for the first time, misalignments between first and second layer are measured. At this point, using the positioning system, the registered misalignments become the desired displacement to apply to the roll (Outputs) in order to print the next second layer in the right position with respect to the first layer. Consequently, by inverting matrix A, desired displacements of the roller are converted into micrometer heads motions (Inputs).

$$
\begin{bmatrix} I_1 \\ . \\ . \\ . \\ I_5 \end{bmatrix} = \begin{bmatrix} 0.00 & -110.61 & 93.56 & 109.85 & -126.89 \\ 0.00 & 0.91 & -0.34 & 0.23 & 0.34 \\ 0.00 & -10.00 & 10.00 & 10.00 & -10.00 \\ -0.64 & -59.11 & 49.99 & 58.71 & -67.83 \\ -0.64 & -59.11 & 50.31 & 58.71 & -68.15 \end{bmatrix} \times \begin{bmatrix} O_1 \\ . \\ . \\ . \\ O_5 \end{bmatrix}
$$

Figure 72: Matrix Equation used to convert the desired print roll displacements into micrometer heads motions. [I] represents the micrometer heads motions to introduce in order to achieve the desired displacements of the roller [O].

Theoretically speaking, after having adjusted the position and the orientation of the print roller, by inserting the computed inputs, the resulting quality should lie within the resolution plus the accuracy of the micrometer head, which in this case ranges within 3.5μm to 5μm according to the different micrometer head used (see paragraph 5.4). In actual systems, the expected error will be larger, due to the not perfect repeatability of the system and the presence of inevitable casual errors.

CHAPTER 7 – Flat Stamp Fabrication[24]

The following chapter is an excerpt from Yufei Zhu's thesis [24]. The section below briefly describes the new stamp fabrication device. For more details, the reader is referred to Yufei Zhu's thesis [24].

7.1 Updated Flat Stamp Fabrication Device

The new stamp fabrication device, shown in Figure 73, is a modification of the old device described in section 3.1. Improvements of this new design include:

- The wafer can be changed easily and quickly aligned.
- Flatness of stamp is at the level of microns.
- The backing plate is mechanically aligned during stamp fabrication.
- Both vacuum chucks used in this device can be disassembled to remove excess PDMS.
- The machine is capable of maintaining low pressure in the internal area during mold filling.
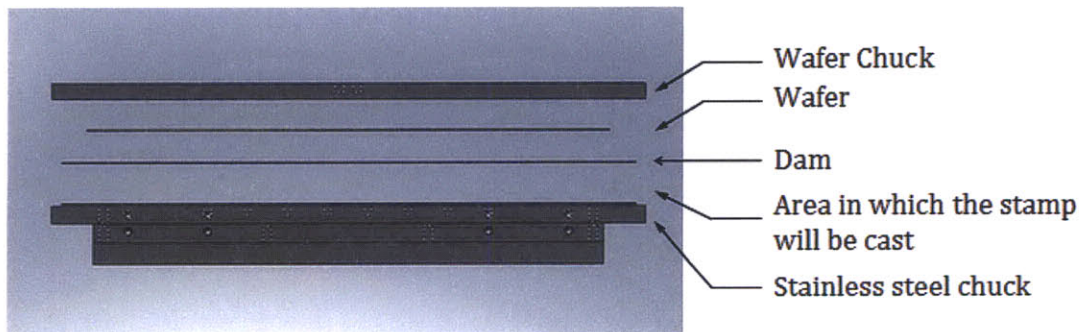

Figure 73: Schematic Illustration of the Casting Machine

7.2 Wafer Chuck

The wafer chuck holds the wafer with a vacuum. The wafer chuck (shown in Figure 74) has concentric grooves, to account for PDMS leaks during the casting process. Another circular channel located outside the grooves prevents PDMS from leaking into vacuum area below the wafer. PDMS is injected through a hose.
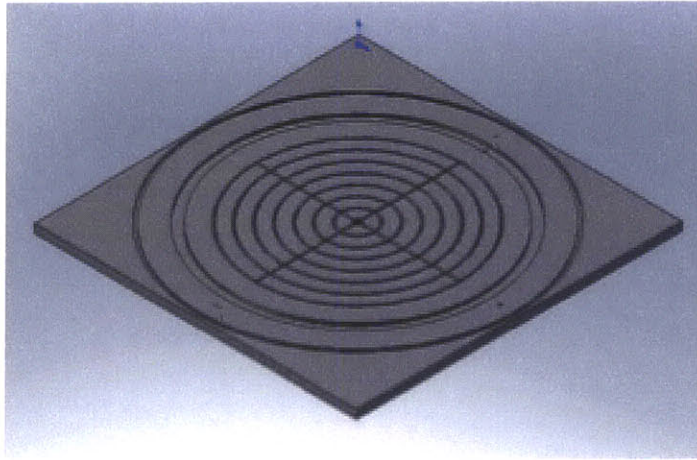
Figure 74: 3D Model of Wafer Chuck for 12" wafer [24].

7.3 Stainless Steel Vacuum Chucks

Stainless Steel (SS) Chucks are used to hold the backing plate (SS Sheet) onto which PDMS adheres. For more details about the design of the chucks, please refer Yufei Zhu's thesis [24].
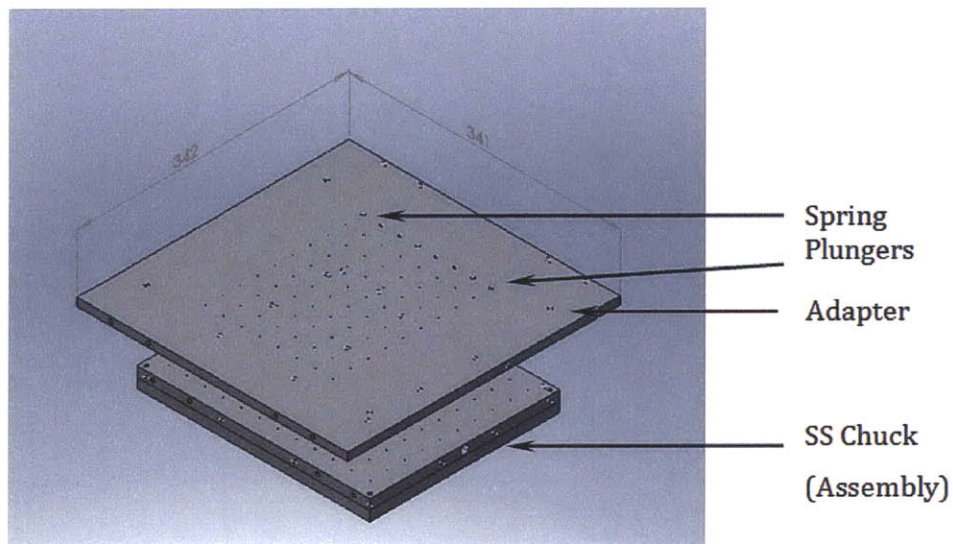
Figure 75: 3D Model of Adapter of SS Chuck for 200mmx200mm Stamp Fabrication [24].

7.4   Assembly of Stamp Fabrication Device

Assembly of the stamp fabrication device follows the method mentioned in Chapter 3.1. And the 3D model of the assembled device is shown in Figure 76. The wafer chuck is represented by a wireframe for clear view inside the structure. Two other clamping bars will be added during stamp fabrication. The location of clamping bar is determined by the location of threaded-holes at the sidebar.

Figure 76: 3D Model of Assembly for 12" wafer (exploded view). The wafer chuck is represented by a wireframe for a clearer view inside the structure [24].

CHAPTER 8 – Multilayer Printing with Updated Roll-to-Roll System [29]

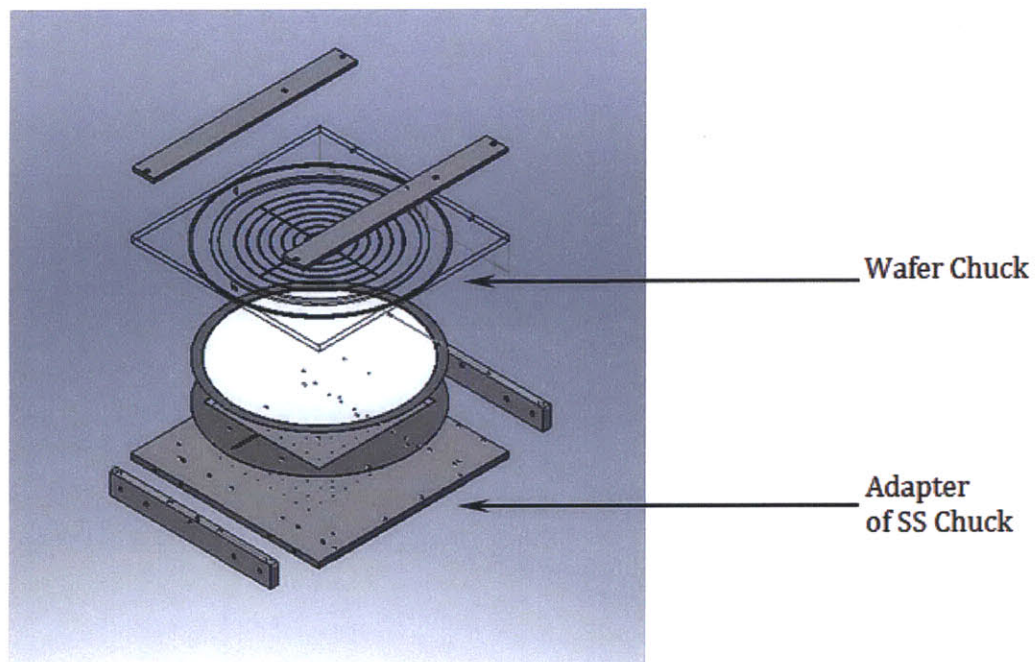The following chapter is an excerpt from Wenzhuo Yang's thesis [29]. The section below briefly describes the multi layer printing process. For more details, the reader is referred to Wenzhuo Yang's thesis [29].

8.1   Introduction of Multi-Layer Printing Process

The primary target of multi-layer printing is to print the second layer of thiol onto the substrate, on top of the first printed layer. In order to use the updated R2R machine to realize multi-layer printing, continuous feedback of the registration is a must. The basic process of two-layer printing in this project is to print the first layer using the updated R2R machine without any alignment control. Then the substrate is wound back and alignment mark on the substrate is found with the help of a camera to align the web position. After that, the second layer is printed for a certain section of the web, the machine is stopped and the misalignment between two layers is again measured and the rollers adjusted correspondingly using the precision positioning system. As a result, after a few iterative steps, the second layer printing should be aligned with the first layer.

While the above description gives a general idea of the process; some critical parts are detailed below:

1. After the first layer printing, the substrate will not be etched. That means although the substrate has the features that looks like the picture shown in Figure 77, those features are not visible. So, marking the general position of each section of pattern is necessary for the etching in the future. The seam between each section of pattern is due to the area with no stamp on the print roller.
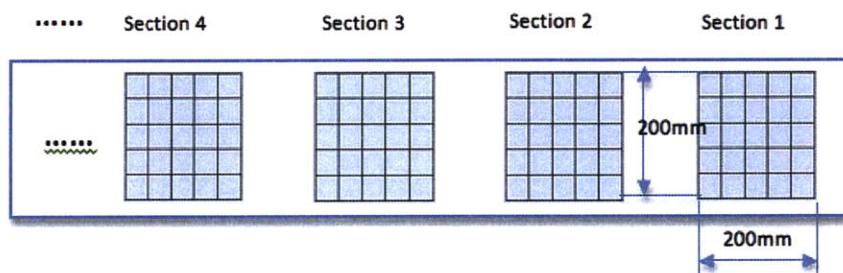

Figure 77: Position of Patterns after First Layer Printing [29].

91

2. After winding back the printed substrate, the impression roller is translated up a certain distance using micrometer head to disengage it from the print roller. Then, the substrate is wound forward with tension maintained by the torque of the driving motor in the collector module, until the section 1 passes through the print roller (shown in Figure 78). The machine is stopped, keeping the position and tension of the substrate unchanged, and the two cameras are used to find the marks at the edges of section 1. Currently, Nano Terra does not have the capability to make alignment marks on the stamp, so the pixel at the edge of the substrate is used as the mark to align the position, and brushing the etchant onto the substrate, those pixels are developed.
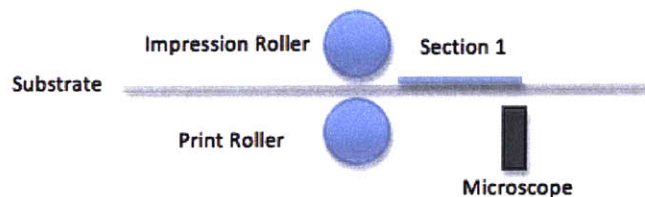

Figure 78: Alignment of the First Layer [29].

3. Adjust two cameras, one at the front of the web and the other at the back, to the position where the "mark pixel" is right at the center of the microscope (see Figure 79). Then, lock the microscopes on the optical table. Since the 200mmx200mm patterns are periodically printed on the substrate, as soon as the microscope shows the "mark pixel" at the corners, we know that the roller has rotated $360°$ and the substrate has just floated the length of the perimeter of the print roller, which means the relative position of the print roller and the substrate is traceable.
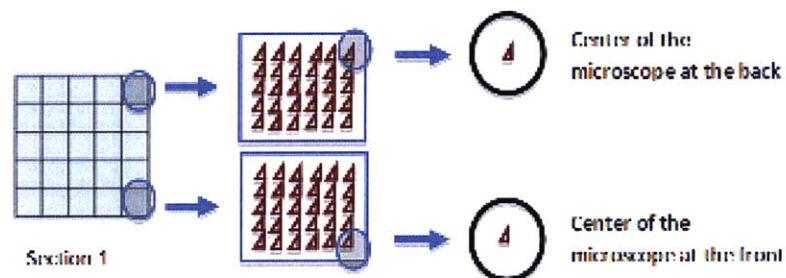

Figure 79: Using Microscope to Align the Position of the Substrate[29].

4. Now, the position of the substrate and the roller is fixed. The impression roller is moved down to the upper surface of the print roller with the substrate in between. We do not want to lose the calibrated position of the substrate by pressing the impression roller onto its surface. So we lock the

feeding and collection rollers and let the impression roller stretch the substrate. As soon as the impression roller and the print roller can hold the substrate, the feeding and collection rollers may be loosened.

5. Start the machine to print the second layer on section 2 and then develop the pixels. Align the "mark pixel" right at the center of the camera, to determine the relative position of the print roller and the substrate. Measure the displacement of two layers and adjust print roller to compensate misalignment. For example, in Figure 80, the x displacement could be adjusted by rotating the roller in angle of X/R; Y displacement could be adjusted by moving the print roller Y units across the printing direction.

Y

Second Layer

First Layer

X

Along the Printing Direction
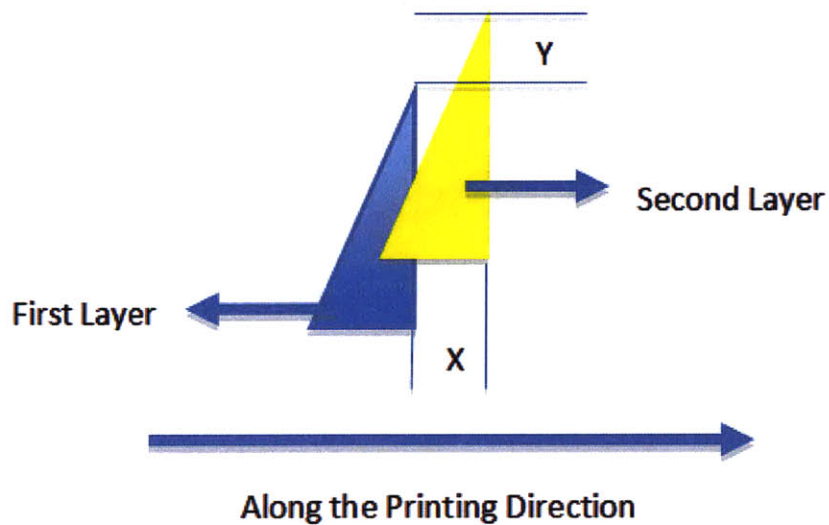
Figure 80: Adjustment of Second Layer printing [29].

6. Ideally, the second layer printing on section 3 should align with the feature on the first layer. If not, re-adjust the print roller and keep printing on section 4. Basically, the machine stops after every printing on each section, align the "mark feature", monitor the overlap of two layers and make adjustment if needed.

CHAPTER 9 – Conclusions and Future Work

9.1 Conclusions

The roll-to-roll machine built in 2008 proved the feasibility of single-layer microcontact printing at speeds as high as 400 feet per minute. However, for microcontact printing to be an industry-competitive solution, it was necessary to demonstrate a high-precision multi-layer printing capability. Keeping this goal in mind, several modifications were made to the machine, in order to test this capability of microcontact printing within a limited budget and time frame.

- o *Flat Stamp Fabrication Machine:* This machine was designed and built to fabricate a flat PDMS stamp and to overcome poor print quality due to stamps with high thickness variation that were manufactured using the previously used injection molding process. This new machine can fabricate stamps with a thickness variation of merely ±16μm.

- o *Wrapping System:* Once the flat stamp is cast on a metal backing plate, it is wrapped on the print roller. The wrapping system must minimize stamp distortions during wrapping. The process must also be repeatable, and must guarantee a precision of distortion error within a few microns. The new wrapping system makes use of a custom designed magnetic roller and a pin-slot alignment mechanism to achieve high-precision and repeatable wrapping. Preliminary experiment shows that wrapping can be achieved with an absolute misalignment of 75 microns between the backing plate and the roller.

- o *Precision Positioning System:* The previous configuration of the roll-to-roll machine did not allow adjustment of the position of the print roller relative to the substrate (web), thus rendering multi-layer printing incapable of achieving high resolution. Thus, a five-axis high-resolution flexure-based system to control the position of the print roller was designed and calibrated to enable an open-loop control to help achieve good quality multi-layer printing. Using this system, the print roller can be positioned and oriented with high repeatability, 2.5μm accuracy, and 2.5μm resolution. Calibration of the precision positioning showed that the five axes are coupled, and in the worst case, this coupling is 8%.

- o *Impression Roller:* The impression roller is located above the print roller. The vertical motion of the impression roller was not repeatable, resulting in lack of control of the final print quality, due to variable pressure. Thus, a

new shaft, plate, and precision linear bearings, were used to improve repeatability.

○ *Multi-Layer Printing Experiments:* Implementing all of the above improvements, multi-layer experiments were conducted, which revealed that the deformation of the printed output was limited to an average of 3.8%. In addition, a ±75 micron misalignment was achieved between two-layers.

9.2   Future Work

The above results are based on preliminary experimentation. Also, given the limited time frame and budget, certain components could not be improved, or introduced. Following is the list of improvements we believe will deliver even better results as far as multi-layer printing is concerned:

○ *Stamp Fabrication:* Currently, the positioning of the backing plate in the flat stamp machine is not high precision, introducing significant uncertainty in the location of the stamp on the backing plate. A better mechanical positioning system, preferably replacing spring plungers with precision dowel pins, should be used.

○ *Wrapping System:* The magnetic print roller is considerably heavy. The current wrapping process is entirely manual. The process could benefit from automation. Automation could also prevent the possibility of accidental damage to holes on the backing plate.

○ *Precision Positioning System:* Displacement of the print roller along any axis is a tedious job, and could be easier if digital ones replaced the vertical micrometer heads. Again, automation is essential and a natural progression to introduce a continuous closed-loop control, which will enable very high-precision multi-layer printing.

○ *Impression Roller:* This impression roller currently only establishes correct, uniform contact of the print roller with the web. However, if replaced by another print roller, it could equip the existing machine with the capability to print on both sides of the substrate. However, this requirement will be customer or industry dependent, and consequently may not be immediately pursued.

○ *High-Resolution Cameras:* The low-resolution of the existing cameras limits the result of misalignment between two printed layers to ±75 micron, thus limiting the achievable resolution of multi layer printing. Replacing these cameras,

which provide feedback of the misalignment between two printed layers, with high-resolution ones will help achieve very high-precision multi layer printing.

o *Driving Motor:* A stepper motor drives the print roller. A stepper motor is not ideally suited for this kind of operation, which requires a smooth, uninterrupted, step-free rotation of the print roller, and hence a flow of the web. Thus, a step-less motor should be used in place of the stepper motor.

o *Web Control:* One major obstacle in achieving high-resolution multi layer printing with the current configuration is the lack of web control. The position of the web literally defines the result of multi layer printing, and lack of its control severely handicaps any effort to minimize error in multi layer printing. Thus, controlling the web is of utmost importance and should be a top priority.
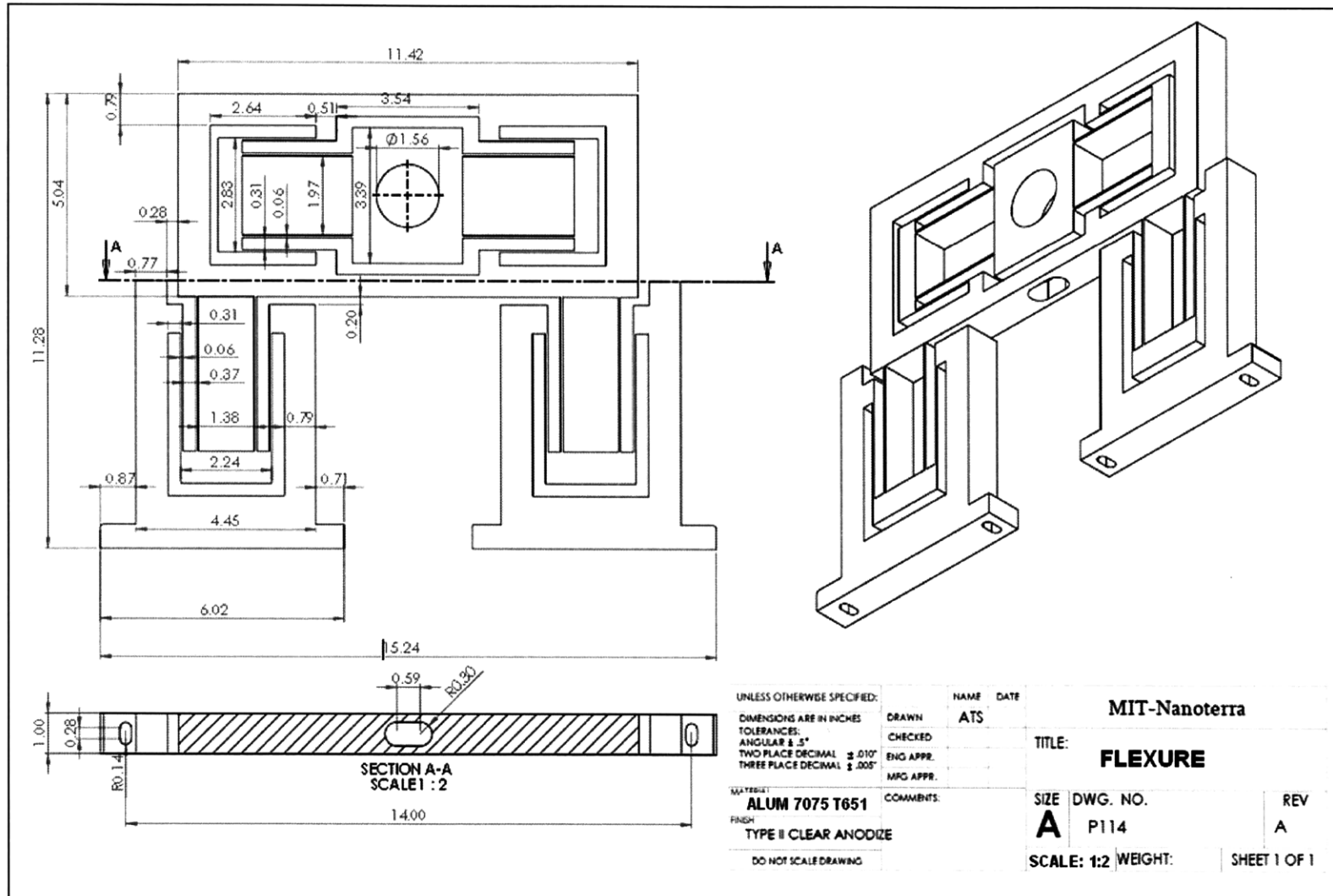
APPENDIX A
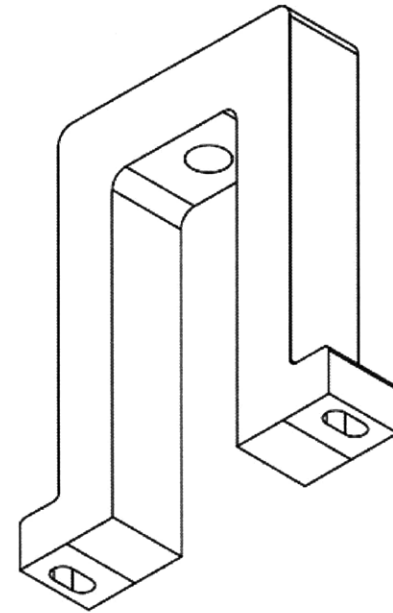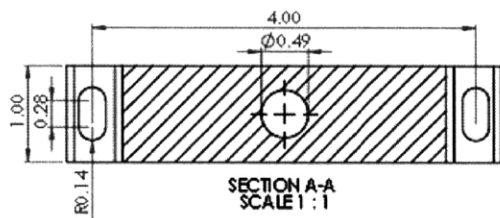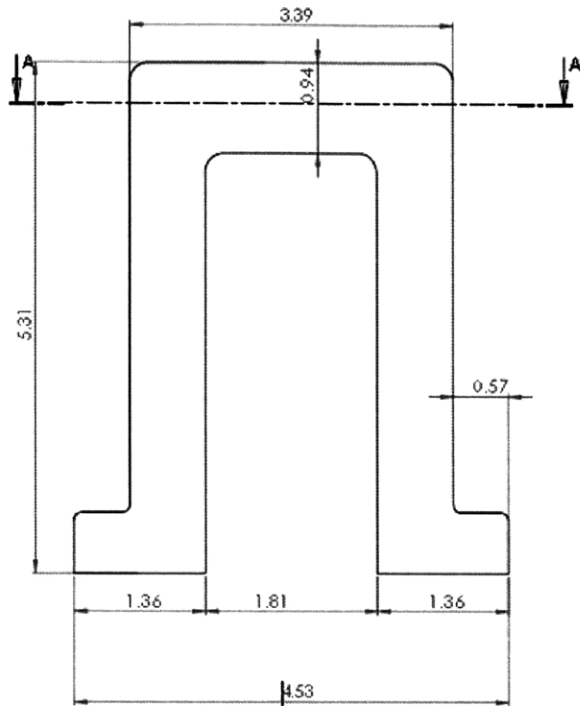
Bill of Material, High Precision Positioning System

nanoterra

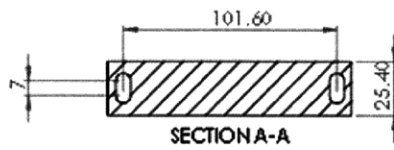| Item	Description	Qty	MFG	Vendor	Part #
1	FLEXURE	2	Kentfab	McMaster	F100
2	HORIZONTAL FIXTURE	2	Kentfab	McMaster	FX110
3	VERTICAL FIXTURE	2	Kentfab	McMaster	FX120
4	FRONTAL FIXTURE	1	Kentfab	McMaster	FX130
5	HORIZONTAL MICROMETER HEAD	2		Mitutoyo	M110
6	VERTICAL MICROMETER HEAD	2		Mitutoyo	M120
7	FRONTAL MICROMETER HEAD	1		Mitutoyo	M130

APPENDIX B

Engineering Drawings, High Precision Positioning System

SECTION A-A
SCALE1 : 2

UNLESS OTHERWISE SPECIFIED:		NAME	DATE	MIT-Nanoterra		
DIMENSIONS ARE IN INCHES	DRAWN	ATS				
TOLERANCES:	CHECKED			TITLE:		
ANGULAR ± .5°	ENG APPR.			**FLEXURE**		
TWO PLACE DECIMAL ± .010"						
THREE PLACE DECIMAL ± .005"	MFG APPR.					
MATERIAL	COMMENTS:			SIZE	DWG. NO.	REV
ALUM 7075 T651				**A**	P114	A
FINISH						
TYPE II CLEAR ANODIZE						
DO NOT SCALE DRAWING				SCALE: 1:2	WEIGHT:	SHEET 1 OF 1

99

3.39

0.94

5.31

0.57

1.36 1.81 1.36

4.53

SECTION A-A
SCALE 1 : 1

4.00

Ø0.49

1.00

0.28

R0.14

UNLESS OTHERWISE SPECIFIED:		NAME	DATE	MIT-Nanoterra		
DIMENSIONS ARE IN INCHES	DRAWN	ATS				
TOLERANCES: ANGULAR ± .5° TWO PLACE DECIMAL ± .010" THREE PLACE DECIMAL ± .005"	CHECKED			TITLE: VERTICAL FIXTURE		
	ENG APPR.					
	MFG APPR.					
MATERIAL ALUM 6061 T651	COMMENTS:			SIZE A	DWG. NO. P114	REV A
FINISH TYPE II CLEAR ANODIZE						
DO NOT SCALE DRAWING				SCALE: 1:1	WEIGHT:	SHEET 1 OF 1

SECTION B-B

SECTION A-A

References

[1] Xia, Y. and Whitesides, G. M., 1998, "Soft Lithography", Annual Review Mater. Sci. 1998. 28:153–84.

[2] Nano Terra Inc, <http://www.nanoterra.com/i/self_assembly_diagram_1.gif>. Accessed 8/1/2008.

[3] Michel, B. et al., 2000, "Printing Meets Lithography: Soft Approaches to High resolution Patterning", IBM Journal of Research and Development, 45(5).

[4] Stagnaro, A., "Design and Development of a Roll-to-Roll Machine for Continuous High-Speed Micro-contact Printing." Massachusetts Institute of Technology, 2008.

[5]. Z.-Q. Gong and K. Komvopoulos, "Effect of surface patterning on contact deformation of elastic-plastic layered media." Journal of Tribology, 125(1):16-24, 2003.

[6] K. L. Johnson. Contact Mechanics. Cambridge University Press, 1987.

[7] J. N. Israelachvili. Intermolecular and surface forces. Academic Press, 2003.

[8] K. L. Johnson, K. Kendall, and A. D. Roberts. Surface energy and the contact of elastic solids. Proceedings of the Royal Society of London Series A, Mathematical and Physical Sciences, 324(1558):301-313, 1971.

[9] M. Forster, W. Zhang, A. J. Crosby, and C.M. Stafford. A multilens measurement platform for high-throughput adhesion measurements. Measurement Science and Technology, 16(1):81-89, 2005.

[10] M. K. Chaudhury and G. M. Whitesides. Direct measurement of interfacial interactions between semispherical lenses and flat sheets of poly(dimethylsiloxane) and their chemical derivatives. Langmuir 7(5):1013-1025, 1991.

[11] A. A. Griffith. The phenomena of rupture and flow in solids. Philosophical Transactions of the Royal Society of London. Series A, Containing Paper of a Mathematical or Physical Character, 221:163-198, 1921.

[12] D. Maugis and M Barquins. Fracture mechanics and the adherence of viscoelastic bodies. Journal of Physics D: Applied Physics, 11(14):1989-2023, 1978.

[13] Brian Cotterell, Gordon Williams, John Hutchinson, and Michael Thouless. Announcements of a round robin on the analysis of the peel test. International Journal of Fracture, 114(3):9-13, 2002.

[14] Laser Triangulation Sensors, <Http:// www.sensorland.com>, Accessed on 08/1/2009.

[15] Interferometry, <Http://www.wikipedia.com> accessed on 08/1/2009.

[16] Alexander H. Slocum, Precision Machine Design, Michigan: Society of Manufacturing Engineers Dearborn, 1992.

[17] MTI instrument Inc. <Http://www.mtiinstruments.com/>, Optical Fiber, accessed on 08/2009.

[18] Giallorenzi et al., Optical Fiber Sensor Technology, IEEE J. Auantum Electron., Vol. QE-18, No.4 1982,pp.

[19] Pawley JB (editor) (2006). Handbook of Biological Confocal Microscopy (3rd ed.). Berlin: Springer.

[20] Khanna,K; "Analysis of the Capabilities of Continuous High-Speed Microcontact Printing"; Massachusetts Institute of Technology, 2008

[21] Shen, Shawn, "Design and Analysis of High-speed Continuous Micro-Contact Printing". Massachusetts Institute of Technology. August 19, 2008.

[22] Sriram Krishnan, "On the Manufacture of Very Thin Elastomeric Films by Spin-Coating", Massachusetts Institute of Technology. September 2007.

[23] Con-Focal Microscopy, <Http://www.wikipedia.com>, accessed on 08/1/2009

[24] Zhu, Yufei. "Design and Manufacturing of High Precision Roll-to-Roll Multi-layer Printing Machine- Machine Upgrade". Massachusetts Institute of Technology. August 18, 2009.

[25] Smith, S.T., Flexures: elements of elastic mechanisms, Amsterdam: Gordon & Brach, 2000.

[26] R. V. JONES, Some uses of elasticity in instrument design, J. SCI. INSTRUM., Vol. 39, 1962.

[27] R. V. JONES, Some parasitic deflexions in parallel spring movements, 1955.

[28] P H Sydenham, Elastic design of fine mechanism in instruments, Sci. Instrum., Vol. 17, 1984.

[29] Yang, Wenzhuo, "Design and Manufacturing of High Precision Roll-to-Roll Multi-layer Printing Machine- Measurement and Experiment". Massachusetts Institute of Technology. August 18, 2009.

[30] Datar, Charudatta, "Development Of High Precision Elastomeric-Stamp Wrapping System For Roll-To-Roll Multi-Layer Microcontact Printing". Massachusetts Institute of Technology. August 18, 2009.

[31] Mitutoyo America Corporation www.mitutoyo.com.